BAŞKENT UNIVERSITY
INSTITUTE OF SCIENCE AND ENGINEERING
DEPARTMENT OF MECHANICAL ENGINEERING
MASTER OF SCIENCE IN MECHANICAL ENGINEERING

THE EFFECTS OF BUILDING DIRECTION ON THE MECHANICAL PROPERTIES OF TI6AL4V PARTS MANUFACTURED BY ELECTRON BEAM MELTING

BY

AHMET ERDEM BOZGÜL

MASTER OF SCIENCE THESIS

ANKARA - 2023

BAŞKENT UNIVERSITY
INSTITUTE OF SCIENCE AND ENGINEERING
DEPARTMENT OF MECHANICAL ENGINEERING
MASTER OF SCIENCE IN MECHANICAL ENGINEERING

THE EFFECTS OF BUILDING DIRECTION ON THE MECHANICAL PROPERTIES OF TI6AL4V PARTS MANUFACTURED BY ELECTRON BEAM MELTING

BY

AHMET ERDEM BOZGÜL

MASTER OF SCIENCE THESIS

ADVISOR

PROF. DR. SAMİ KARADENİZ

ANKARA – 2023

BAŞKENT UNIVERSITY

INSTITUTE OF SCIENCE AND ENGINEERING

This study, which was prepared by Ahmet Erdem BOZGÜL, for the program of Mechanical Engineering Master of Degree with Thesis, has been approved in partial fulfillment of the requirements for the degree of MASTER OF SCIENCE in the Mechanical Engineering by the following committee.

Date of Thesis Defense: 06 / 01 / 2023

Thesis Title: The Effects of Building Direction on the Mechanical Properties of TI6AL4V Parts Manufactured by Electron Beam Melting

Examining Committee Members	**Signature**
Prof. Dr. SAMİ KARADENİZ	…….
Prof. Dr. MÜFİT GÜLGEÇ	…….
Prof. Dr. SEDAT BAYSEÇ	…….

APPROVAL

Prof. Dr. Faruk ELALDI

Director, Institute of Science and Engineering

Date: … / … / ……..

BAŞKENT ÜNİVERSİTESİ

FEN BİLİMLER ENSTİTÜSÜ

YÜKSEK LİSANS ÇALIŞMASI ORİJİNALLİK RAPORU

Tarih: 10 / 01 / 2023

Öğrencinin Adı, Soyadı: Ahmet Erdem BOZGÜL

Öğrencinin Numarası: 22010514

Anabilim Dalı: Makine Mühendisliği Anabilim Dalı

Program: Tezli Yüksek Lisans Programı

Danışmanın Unvanı/Adı, Soyadı: Prof. Dr. Sami KARADENİZ

Tez Başlığı: The Effects of Building Direction on the Mechanical Properties of TI6AL4V Parts Manufactured by Electron Beam Melting

Yukarıda başlığı belirtilen Yüksek Lisans çalışmamın; Giriş, Ana Bölümler ve Sonuç Bölümünden oluşan, toplam 85 sayfalık kısmına ilişkin, 10/01/2023 tarihinde şahsım tarafından Turnitin adlı intihal tespit programından aşağıda belirtilen filtrelemeler uygulanarak alınmış olan orijinallik raporuna göre, tezimin benzerlik oranı % 14'dür. Uygulanan filtrelemeler:

1. Kaynakça hariç
2. Alıntılar hariç
3. Beş (5) kelimeden daha az örtüşme içeren metin kısımları hariç

"Başkent Üniversitesi Enstitüleri Tez Çalışması Orijinallik Raporu Alınması ve Kullanılması Usul ve Esaslarını" inceledim ve bu uygulama esaslarında belirtilen azami benzerlik oranlarına tez çalışmamın herhangi bir intihal içermediğini; aksinin tespit edileceği muhtemel durumda doğabilecek her türlü hukuki sorumluluğu kabul ettiğimi ve yukarıda vermiş olduğum bilgilerin doğru olduğunu beyan ederim.

Öğrenci İmzası:…….

ONAY

Tarih: 10 / 01 / 2023

Prof. Dr. Sami KARADENİZ

……

ACKNOWLEDGEMENTS

I would like to express my gratitude to my advisor, Prof. Dr. Sami KARADENİZ for his guidance, support, and valuable advice.

My colleague Mustafa Anıl YILDIRIM, Dr. Reha GÜNAY, Hakan HAFIZOĞLU, and Hüseyin Emrah KONOKMAN for their support in test processes.

I am appreciative to my mother Vijdan BOZGÜL, my father Mustafa BOZGÜL and my elder sister İrem BOZGÜL for their effort through my childhood, and education period.

Lastly, I am grateful to my company Turkish Aerospace for providing me chance to complete my study.

ABSTRACT

AHMET ERDEM BOZGÜL

THE EFFECTS OF BUILDING DIRECTION ON THE MECHANICAL PROPERTIES OF TI6AL4V PARTS MANUFACTURED BY ELECTRON BEAM MELTING

Baskent University Institute of Science and Engineering

Department of Mechanical Engineering

2023

In recent years, the additive manufacturing technology is used in many platforms like helicopters, airplanes, cars etc. The additive manufacturing technology has widespread advantages because of the low manufacturing costs and relatively short manufacturing time compared with the conventional manufacturing methods. The materials, the manufacturing technique and processes affect the material form that is used in proper platform. In the industrial sector, there are different additive manufacturing technologies such as Electron Beam Melting, Laser Beam Melting, Laser Metal Deposition, Laser Coating, and Additive Manufacturing. Among them, the manufacturing technique which uses powder bed technique like Electron Beam Melting technology is preferred in industry since the manufacturing technique is more suitable to produce parts having better surface quality, complicated geometric shaped products for the various designs. However, the additive manufacturing methods have some disadvantages such as the presence of the residual stresses and deformations of the end products.

In this thesis, both the static and dynamic mechanical properties of Ti6Al4V parts that were produced in vertical and horizontal building directions by the electron beam melting method were carried out experimentally and the results were compared with the corresponding properties of Ti6Al4V parts produced by conventional methods. In order to investigate the mechanical properties; the surface roughness tests; tensile tests and the Split-Hopkinson high strain rate compression tests of the parts were carried out. The differences in the mechanical properties of the samples manufactured in different building directions were investigated and the effects of microstructure on these properties were studied by examining the internal microstructure texture with a microscope technology.

As a result of this study, it is found that the manufacturing direction affects the static and dynamic mechanical properties of the Ti6Al4V parts. The vertically manufactured parts have higher Yield Strength, Ultimate Tensile Strength and Elastic Modulus compared to horizontally manufactured parts. In addition, the parts that are manufactured by Electron Beam Melting method have lower Rockwell C hardness value than pure Ti6Al4V parts and also have some porosities inside the microstructure. Besides the manufacturing direction the porosities and defects have also effects on the mechanical properties of the parts.

KEYWORDS: Additive Manufacturing, Electron Beam Melting, different building direction, static and dynamic mechanical properties, Ti6Al4V

ÖZET

AHMET ERDEM BOZGÜL

ÜRETİM YÖNÜNÜN ELEKTRON IŞINI ERİTME İLE ÜRETİLEN TI6AL4V PARÇALARININ MEKANİK ÖZELLİKLERİNE ETKİLERİ

Başkent Üniversitesi Fen Bilimleri Enstitüsü

Makine Mühendisliği Anabilim Dalı

2023

Eklemeli imalat teknolojisi son yıllarda helikopter, uçak, araba vb. birçok platformda kullanılmaktadır. Eklemeli imalat teknolojisi, geleneksel imalat yöntemlerine kıyasla düşük imalat maliyetleri ve nispeten daha kısa imalat süresi nedeniyle yaygın avantajlara sahiptir. Malzemeler, üretim tekniği ve süreçleri, uygun platformda kullanılan malzeme formunu etkilemektedir. Sanayi sektöründe Elektron Işını Eritme, Lazer Işını Eritme, Lazer Metal Biriktirme, Lazer Kaplama ve Eklemeli İmalat gibi farklı eklemeli imalat teknolojileri bulunmaktadır. Bunlardan Elektron Işını Eritme teknolojisi gibi toz yatak tekniğini kullanan üretim tekniği, çeşitli tasarımlar için daha iyi yüzey kalitesine sahip parçaları, karmaşık geometrik şekilli ürünleri üretmeye daha uygun olduğu için endüstride tercih edilmektedir. Ancak, eklemeli imalat yöntemlerinin, nihai ürünlerin kalıntı gerilmelerinin ve deformasyonlarının varlığı gibi bazı dezavantajları vardır.

Bu tezde, elektron ışını eritme yöntemi ile dikey ve yatay üretim yönlerinde üretilen Ti6Al4V parçalarının hem statik hem de dinamik mekanik özellikleri deneysel olarak incelenmiş ve sonuçlar, geleneksel yöntemlerle üretilen Ti6Al4V parçalarının karşılık gelen özellikleri ile karşılaştırılmıştır. Mekanik özellikleri incelemek için; yüzey pürüzlülük testleri; parçaların çekme testleri ve Split-Hopkinson yüksek gerinim hızı testleri yapılmıştır. Farklı bina yönlerinde üretilen numunelerin mekanik özelliklerindeki farklılıklar araştırılmış ve mikroyapının bu özellikler üzerindeki etkileri mikroskop teknolojisi ile iç mikroyapı dokusu incelenmiştir.

Bu çalışma sonucunda, üretim yönünün Ti6Al4V parçalarının statik ve dinamik mekanik özelliklerini etkilediği gözlemlenmiştir. Dikey olarak üretilen parçalar, yatay olarak üretilen parçalara kıyasla daha yüksek Akma Mukavemeti, Nihai Çekme Mukavemeti

ve Elastik Modülüne sahiptir. Elektron Işını Eritme yöntemi ile üretilen parçaların, saf Ti6Al4V parçalara göre Rockwell C sertlik değeri daha düşüktür ve mikro yapı içinde bazı gözeneklere sahiptir. Üretim yönünün yanı sıra gözenekler ve kusurlar da parçaların mekanik özellikleri üzerinde etkilidir.

ANAHTAR KELİMELER: Katmanlı Imalat, Elektron Işını Eritme, Farklı üretim yönü, statik ve dinamik mekanik özellikler, Ti6Al4V

TABLE OF CONTENTS

LIST OF TABLES

LIST OF FIGURES

LIST OF SYMBOLS AND ABBREVIATIONS

FEM	Finite Element Method
STL	Stereolithography Format
SLM	Selective Laser Melting
EBM	Electron Beam Melting
SLS	Selective Laser Sintering
DMLS	Direct Metal Laser Sintering
EBFFF	Electron Beam Free Form Fabrication
LENS	Laser Engineered Net Shaping
DMD	Direct Metal Deposition
LMD	Laser Metal Deposition
FDM	Fused Deposition Modeling
kg	Kilogram
h	Hour
Al	Aluminum
Ti	Titanium
W	Watt
kW	Kilowatt
CAD	Computer Aided Design
PBF	Powder Bed Fusion
s	Second
g	Universal Gravitational Constant
HIP	Hot Isostatic Pressing
Ni	Nickel
Si	Silisium
Mg	Magnesium
Sc	Scandium
Nb	Niobium
Zr	Zirconium
Sn	Stannum
Mo	Molybdenum
Co	Cobalt
Cr	Chromium
3DP	Binder Jetting
IJP	Inkjet Printing
MJM	Multi-Jet Modeling
BPM	Ballistic Particle Manufacturing
LOM	Laminated object manufacturing
SFP	Solid Foil Polymerization
SLA	Stereolithography Additive Manufacturing
SGC	Solid Ground Curing
LTP	Liquid Thermal Polymerization
α	Alpha
β	Beta
HCF	High Cycle Fatigue Test
LCF	Low Cycle Fatigue Test
ε_t	Total Strain
ε_p	Plastic Strain

ε_e	Elastic Strain
X	x-direction in coordinate system
Y	y-direction in coordinate system
Z	z-direction in coordinate system
YS	Yield Strength
UTS	Ultimate Tensile Strength
HRC	Hardness Rockwell C
$R_{p0.2}$	Elongation Point
R_m	Tensile strength
SHPB	Split-Hopkinson Pressure Bar

1. INTRODUCTION

Additive manufacturing technology is used in industrial technologies and it provides manufacturing of complex products and low-cost products with less effort. In addition, the industry demands the parts that are produced with additive manufacturing technology have similar characteristics to products, which are produced with traditional methods. The metals like titanium, steel, and aluminum can be used within this technology. Therefore, companies try to use additive manufacturing technology to decrease both the cost and manufacturing time of the products. Although additive manufacturing technology cannot compete with subtractive manufacturing yet, its applications are rapidly spreading in many industries such as the aviation industry, automobile industry, medicine industry, etc. [1]. Additive manufacturing has some advantages according to subtractive manufacturing like design freedom, integrated design, the flexibility of production without any product-specific tool, and a decrease in production time [2]. The production can be made by using direct 3D data, so it provides a reduction in tool designs, production time required in the requested time, and effort to design. In addition, the 3D CAD data is broken down into 2D manufacturing steps [3]. Therefore, complex products are produced without any difficulty. However, in some situations, a number of support parts is required to build the products [3]. In addition, another advantage of additive manufacturing is waste materials like burrs and sawdust which are much less occur while manufacturing. Therefore, this technology is environmentally friendly compared with conventional manufacturing methods.

Additive manufacturing has some disadvantages besides its advantages. Firstly, although by using this technology, complex products can be manufactured, sensitive tolerances may not be provided. Secondly, the surface quality cannot be compared with the conventional methods. In addition, residual stresses, deformations, and porosities have also come into existence. Therefore, additive manufacturing technology is still being tested to specify the design limits and the improvement of complex designs. The test and manufacturing costs are high because of the raw material costs, so before the manufacturing process, the products need to be analyzed and optimized within the 3D design optimizations and simulations [3].

Modeling and simulation studies in the field of additive manufacturing have emerged in parallel with the development of metal parts manufacturing technologies. The main reason is the high price of parts made of metal materials, and researchers begin to need the foresight to reduce experiments. Modeling studies, which are relatively new and have been seriously studied for less than a decade, are supported by software using the general-purpose finite element method (FEM). In this context, although basic studies have been carried out, effective solutions have not been provided for complex and large-sized part geometries. Since this situation is a necessity, special software for additive manufacturing simulations has been developed and it has benefited from shortening the solution times. However, in some situations, mathematical omissions and assumptions that are made during their development cannot be understood properly by practicing engineers or researchers and this prevents them to gain the formation of healthy knowledge [3].

1.1. Literature Survey

In the research reported in Reference [4], in aerospace applications Ti6Al4V titanium alloy components are used for primary and secondary loading locations such as bearings, support brackets, and fittings [4]. The brackets and fittings that are manufactured for experiments for spacecraft applications are shown in Figure 1.1.

Figure 1.1: Ti6Al4V EBM detail parts [4]

The experimental results that are reported in Reference [4], most of the fittings and brackets were designed for worst-case load conditions. The compression tests were

performed to obtain load data of brackets made of Ti6Al4V that are manufactured with EBM method.

The different types of specimens were indicating the Ti6Al4V end fitting assemblies that are manufactured with EBM technology. The specimens were resulted in the failure load at 711 MPa that is close to the specimens that are manufactured with conventional methods. Therefore, the results of the test show that the additive manufacturing technology can be used in aerospace industry because it shows same load results in the bracket and fittings' compression tests [4].

In the V. Chastand, et al. research [5], Ti6Al4V titanium alloy is also tested for the fatigue performances according to ASTM F2924. The specimens are built in the Z axis to reveal the built direction effect on surface roughness and the Hot Isostatic Pressing (HIP) heat treatment [5].

Table 1.1 Test results in V. Chastand et al. research [5]

Type of test	Z axis 650°C/4h Machined/polished	X-Y axis 650°C/4h Machined/polished	Z axis 650°C/4h As-built	Z axis 650°C/4h + HIP Machined/polished
HCF test	12	12	12	12
LCF test	8	8	8	8

The constant stress High Cycle Fatigue Test (HCF) was performed for fatigue and the test results can be seen in Table 1.1. In the study reported in ref [5], the relative stress values were compared with casted and wrought methods changing the different parameters to obtain stress levels [5].

From the results, the observations can be made:

- The build direction has not to affect the fatigue limit of specimens.
- The roughness of the part surface has a crucial effect on the fatigue life of specimens. In addition, the fatigue life is doubled after deburring and polishing process.

- Heat treatment (HIP) process has a crucial impact on the fatigue properties of the specimens. The fatigue properties are increased by 90% after the HIP process compared with stress-relieved specimens [5].

According to the LCH test results, the total strain $\Delta\varepsilon_t/2$ shows the failure amplitude and it is compared with the $\Delta\varepsilon_p/2$ (plastic strain) and $\Delta\varepsilon_e/2$ (elastic strain) relations that are indicated in equation (1.1).

$$\frac{\Delta\varepsilon_t}{2} = \frac{\Delta\varepsilon_p}{2} + \frac{\Delta\varepsilon_e}{2} \tag{1.1}$$

The effect of the heat treatment process HIP can be clearly observed from tests. After the heat treatment, the porosities and the zones that are unmolded are reduced. These samples are going to have much more fatigue life than stress-relieved samples due to the low number of defects [5].

In the work of Alok Gupta et al. [6], the tensile properties, strain rate dependence, temperature, roughness and build direction of the Ti6Al4V EBM-processed specimens that were studied. In their research [6], Ti6Al4V powder and ARCAM A2XX EBM machine with standard process parameters were used. For the tensile tests, the vertical and horizontal built direction was used. However, in the vertical direction, two different types of specimens; as built and machined were used. The manufacturing directions are shown in Figure 1.2.

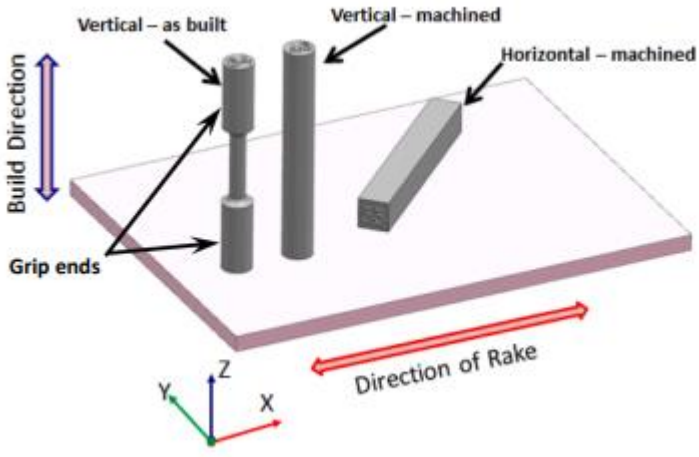

Figure 1.2: Manufacturing orientation specimens in Alok Gupta et al. study [6]

According to the experimental results of the Gupta et al. research [6], the 0.2% Proof Strength assumption was used in tensile tests. YS and UTS and material ductility results are shown in Table 1.2. The VM, HM and VA identification numbers represent vertically manufactured, horizontally manufactured and vertically as-built respectively.

Table 1.2: Tensile results of specimens in Gupta et al. study [6].

Test Identification Number (#)	Temperature (°C)	Strain Rate (SR) – $\dot{e}$ (s^{-1})	YS (MPa)	UTS (MPa)	Ductility (%)
VM1	20	0.0002	953	1013	8.4
VM2	20	0.0265	1020	1050	6.8
VM3	200	0.0002	708	802	16.6
VM4	400	0.0002	575	691	12.1
VM5	400	0.0265	550	658	15
HM1	20	0.0002	927	1007	12.6
HM2	20	0.0265	1022	1042	12.1
HM3	400	0.0002	506	658	14.5
HM4	400	0.0265	522	648	12.3
VA1	200	0.0002	652	711	3.6
VA2	200	0.002	718	747	2.4
VA3	400	0.002	560	590	1.8
VA4	400	0.0265	547	580	1.7
Annealed Ti-6Al-4V Bar [42]	20	–	861	930	10

In the research [6], according to the results of tensile tests, it was found that horizontally manufactured specimens have higher ductility than vertically manufactured specimens. From the results in Table 1.2, the vertically manufactured specimens have higher YS and UTS values compared to the horizontally and vertically as-built specimens. Therefore, it was stated that the mechanical properties of Ti6Al4V specimens were affected by manufacturing direction. Alok Gupta et al. stated that the tensile results of the specimens were associated with the crack path, porosities, and defects in the microstructure of the parts. It was seen that the crack way was parallel to the loading direction. It caused deflections and strength increases [6].

When the effect of the surface roughness was examined, the staircase effect that is related to thickness, the melted powder surface, and the open pores which occur in the part surface decreased the surface quality. Two different types of specimens were manufactured to study the surface quality on mechanical properties. One of them was machined and the other was as-built. The machining, polishing, and surface processes were done to machined specimens. According to Table 1.2, it is seen that there is a decrease in YS, UTS, and ductility results for VA (as-built) specimens. However, the corresponding values for the machined ones are

significantly higher than that of as-built parts. As a result, it can be concluded that the surface quality has an effect on the mechanical properties of Ti6Al4V [6].

In the S. Gangireddy et al. research [7], the dynamic compression behavior of Ti6Al4V parts for different manufacturing orientations was studied. In this research, Ti6Al4V powder with 15 to 45µm was used and the parts were manufactured horizontally, vertically and 45° for the Split Hopkinson Bar Tests. The manufacturing directions and locations are shown in Figure 1.3.

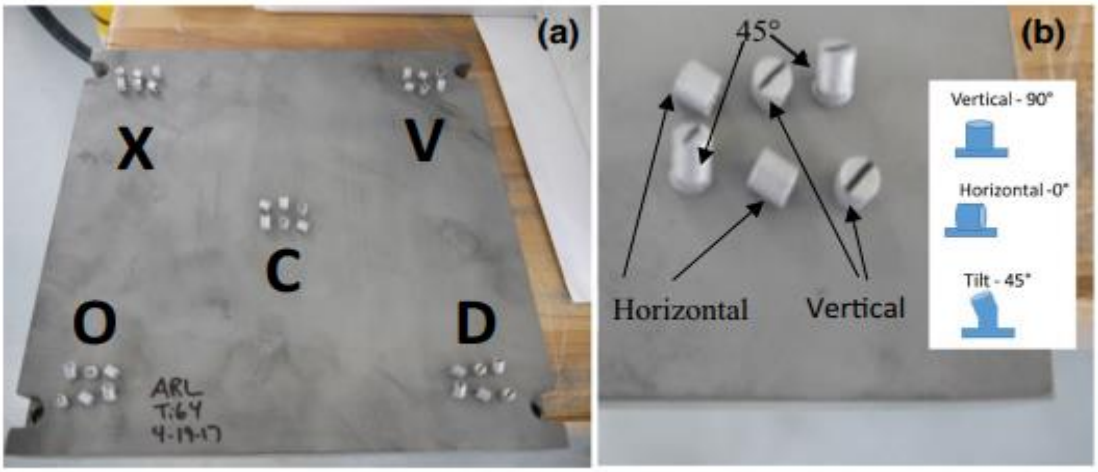

Figure 1.3: (a) The specimens codes of S. Gangireddy et al. research, (b) different manufacturing directions in each location [7]

In the research reported in ref [7], the Split Hopkinson compression test results corresponding to the as-built, residual stress-relieved, and HIP'ped specimens with horizontal, vertical, and 45° built are shown in Figure 1.3, with five different locations which are rear left (X), rear right (V), front left (O), front right (D), and center (C) [7]. As it is seen, both the as-built specimens and the non-residual stress-relieved specimens prove higher strength values which were about 1600–1700 MPa because of their martensitic microstructure. The HIP'ped Ti6Al4V alloy showed strengths values about 1300–1450 MPa at 1000 s^{-1} high strain rate.

The vertically manufactured specimens that are parallel to the loading axis which are same stresses in compression compared to the horizontally manufactured specimens. During the uniaxial compression strength, the shear stresses were directed for the 45° plane due to

dislocation motion. Therefore, 45° built specimens that have slightly higher strength than the horizontally and vertically manufactured specimens. To conclude, in the S. Gangireddy, E. J. Faierson et al. research [7], horizontally and vertically manufactured specimens' dynamic mechanical properties close to each other at higher strain rates, the 45° built specimens' dynamic mechanical properties seem to be slightly higher. In addition, the location of the parts during manufacturing also affects the dynamic mechanical properties [7].

In the research reported in ref [8], the vertical and horizontal Ti6Al4V three specimens were tested in tensile test machine. The average values of YS, UTS of vertical specimens were 1025 MPa and 1130 MPa respectively. However, the average tensile test results of horizontal specimens were 960 MPa and 1065 MPa respectively.

In the Everth Hernandez-Nava research [9], the quasi-static tension tests were subjected to Ti6Al4V test parts manufactured by ARCAM S12 EBM machine to obtain mechanical properties. The manufacturing process parameters of the ARCAM S12 are given in Table 1.3.

Table 1.3: Process Parameters of Everth Hernandez-Nava research [9].

Theme	Current (mA)	Speed (mm/s)	SF	FO (mA)	Line offset (mm)	Line order (mm)	OC (mm)
Net	1.7-3	200	1	0	0.2	1	0.050
Melt	17	500	36	19	0.2	1	0
Wafer	7	1500	–	0	5	–	–
Preheat I	30	14600	–	50	1.2	15	–
Preheat II	38	14600	–	50	1.2	15	–

In the research, vertically and horizontally specimens were used and tested with Hounsfield TX0039 machine. The results of the tests were indicated in Table 1.4.

Table 1.4: Mechanical properties of the tensile specimens from Everth Hernandez-Nava research [9]

Samples	0.2% Y.S. (MPa)	U.T.S. (MPa)	Young Modulus (GPa)	Elongation %
Horizontal	881 ± 8	1040 ± 6	110.0 ± 2.2	16 ± 1
Vertical	923 ± 10	1042 ± 9	116.5 ± 2.8	14 ± 1

Their results revealed that the YS, UTS, E and Elongation values were affected by manufacturing orientation of the specimens.

In the Guillaume Mandil et al. research [10], the Ti6Al4V specimens were manufactured by ARCAM A1 EBM machine with a 60kV voltage, 50mA maximum beam current, and 8000m/s scan speed. The tensile tests were done by using DY 35 tensile test machine. The microhardness of the specimens was measured at 390 HV. The Young's modulus and the UTS value of the specimens reached 114 GPa and 1289 MPa [10].

In the research reported in ref [11], Haize Galarraga et al. use Ti6Al4V gas atomized powder with between 45-150 μm. The specimens were manufactured horizontally and vertically built direction by using an ARCAM EBM machine. The Tensile specimens were machined to obtain better surface quality. The tensile specimens were studied using an Instron 5500R tensile test machine. The tensile test results were given in Table 1.5.

Table 1.5: Average tensile test results of horizontal and vertical test specimens [11].

	Horizontal		Vertical		Cast + annealed
	Average	RSD [%]	Average	RSD [%]	
UTS [MPa]	1066	0.9	1073	2.6	930
YS [MPa]	1006	2.9	1001	2.5	855
el [%]	15.0	12.9	10.8	17.6	12

According to the results, the manufacturing direction has a slightly effect on mechanical properties. In addition, the YS and UTS value of specimens seem higher than traditionally manufactured Ti6Al4V titanium alloy.

In the research of P. Edwards et al [12], the vertical and horizontal built specimens were subjected to dynamic and static mechanical tests to obtain the mechanical properties. The specimens were built by using the EBM method. In the research, it was stated that the porosities and surface quality of the specimens had a directly impact on dynamic and static mechanical properties. According to the results, the YS and UTS values of vertically manufactured specimens were 818 MPa and 851 MPa respectively, however, horizontally manufactured specimens were 783 MPa and 833 MPa. According to the research, the built direction's effect on both dynamic and static mechanical properties was observed [12].

In the research of Formanoir et al. [13], It was stated that the tensile properties and elongation values were increased from 780MPa to 1130MPa and 2.3% to 20% according to the building directions and surface quality processes. In the research, some of the specimens were polished to increase the surface quality after building, to obtain whether the surface roughness has an effect on the mechanical properties or not. The non-polished specimens' YS value resulted in an average of 832 MPa, however, the polished specimens resulted in as average of 1055 MPa. It is seen that the polished specimens resulted in higher YS values compared to non-polished specimens. In addition, the HIP process was done after building, and it was stated that it has a slightly effect on mechanical properties [13].

In the research reported in [14], Zhai et al. compared the LENS and EBM methods for Ti6Al4V parts. The scan power of the LENS and EBM machines was also compared to whether it affected the mechanical properties or not. The input laser power parameter was taken as 330W, then it was increased to 780W. When the scan power was gone up, the YS and UTS of the specimens built by LENS increased from 1005 to 1103 MPa and 990 to 1042 MPa respectively. In the EBM manufacturing trial, the horizontally built specimens changed from 937 to 1006 MPa and 1032 to 1066 MPa, and the vertically built specimens changed to 1001 to 1051 MPa and 1073 to 1116 MPa respectively (See Table 1.6). Zhai et al. concluded that the vertically built specimens have higher YS and UTS values compared to horizontally built specimens [14].

Table 1.6: Average tensile test results of horizontal and vertical test specimens [14]

	YS (MPa)	UTS (MPa)	%EL
B1-horizontal as deposited	1006	1066	15
B1-vertical as deposited	1001	1073	11
B2-horizontal as deposited	973	1032	12
B2-vertical as deposited	1051	1116	15
Solutionized and aged	1039	1294	10

According to the results, the vertically manufactured B specimens had higher mechanical test (YS and UTS) values than the horizontally built B specimens [14].

The research of Hrabe and Quinn [15] investigated that the effects of building direction had a slightly effect on the mechanical properties of Ti6Al4V. The results indicated

that the UTS and YS values of horizontal direction were 983 and 1030 MPa, and the vertical direction was 961 and 1014 MPa. The horizontal building direction elongation was 30% higher than the vertical building direction [15].

In Edwards et al. research [16] both the dynamic and static mechanical properties of Ti6Al4V specimens, which were produced by the ARCAM A1 EBM machine. The horizontal and vertical built specimens have been located in the machine lathe as shown in Figure 1.4.

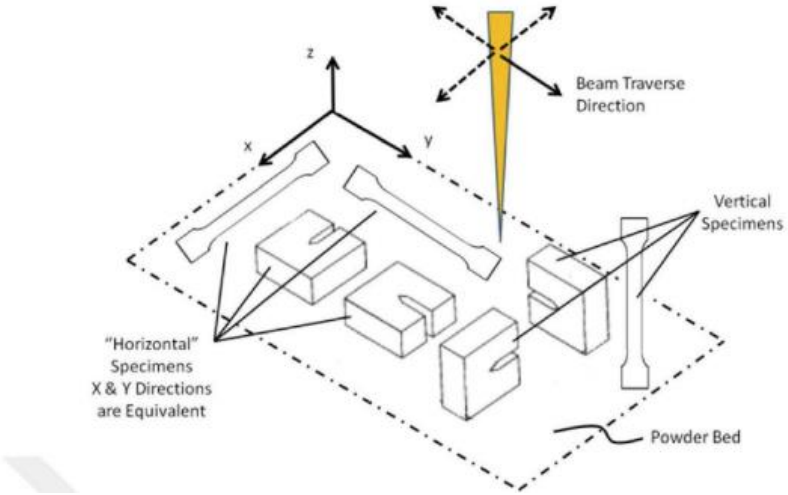

Figure 1.4: Specimen Orientation Schematic in EBM machine [16]

In the research the scan speed was taken as 3 m/s, the input power was taken as 3500W and the process temperature was 700◦C for the vacuum chamber. No HIP process was performed on the specimens after manufacturing. The vacuum temperature was adjusted to the optimal value to decrease the residual stress and not to do stress relief processes. However, it was stated that the porosities and defects in the microstructure still affect the fatigue life of the parts [16]. The results of the tensile tests are shown in Table 1.7. It is seen that the vertically built specimens have higher YS and UTS values than horizontally manufactured specimens.

Table 1.7: Average tensile test results of horizontal and vertical test specimens from Edwards et al. research [16]

	0.2% YS (MPa)	UTS (MPa)	Elongation (%)
Horizontal	833	783	2.7
Vertical	851	812	3.6

In the Wauthle et al research [17] the manufacturing direction effect on the static mechanical properties of specimens was investigated. The three different orientations, vertical, 45°, and horizontal direction, for lattice structures were studied. It was studied on compression and the stiffness value of the 45◦ built specimens was 35% lower than the vertical specimens, however, 45° had nearly the same stiffness value compared to horizontal built specimens [17].

In the research reported in [18], Gong et al. compared the EBM and SLM methods on the mechanical properties of Ti6Al4V specimens. In addition, the process parameters were changed to indicate the parameter effect on mechanical properties. The process parameters of machine were shown in Table 1.8 and Table 1.9Table 1.8.

Table 1.8: SLM process parameters of Gong et al. research [18]

	Scan Speed (mm/s)	Energy Density (J/mm^3)
Parameter 1	960	42
Parameter 2	540	74
Parameter 3	400	100
Parameter 4	1260	32
Parameter 5	1500	27

Table 1.9: EBM process parameters of Gong et al. research [18]

	Beam Current Max (mA)	Speed Function Index	Line Offset (mm)	Focus Offset (mm)
Parameter 1	21	98	0.1	3
Parameter 2	30	60	0.2	15
Parameter 3	20	180	0.2	5

In the research, the Ti6Al4V Grade 23 spherical powder was processed for both manufacturing methods DMLS and EBM by EOS M270 and ARCAM S400 machines. The specimens were built in the vertical direction for both manufacturing methods. The tensile and hardness tests were performed to specimens [18]. The results of the tensile tests are shown in Table 1.10.

Table 1.10: Tensile Properties of Specimens from Gong et al. research [18]

	0.2% YS (MPa)	UTS (MPa)	Elongation (%)	Young's Modulus (GPa)
SLM Specimens	1011	1146	6.5	102
EBM Specimens	954	1012	8.9	121

SLM specimens showed higher YS and UTS values compared to the EBM specimens. However, SLM specimens resulted in lower ductility than EBM specimens although, their microstructure is not fully martensitic [18].

The research of S. T. Yiğitbaşı [19] about the mechanical properties of the vertical and horizontal built directions of Ti6Al4V specimens indicated that the vertically manufactured specimens have better YS and UTS than horizontally manufactured specimens. The vertically manufactured specimens have 1023 MPa UTS, 940 MPa YS, 158 GPa, E, and 10% Elongation. However, horizontally manufactured specimens have 988 MPa UTS, 895 MPa YS, 136 GPa, E, and 15% Elongation. It is clearly seen that; the overall results are similar and, the built direction of the specimens in additive manufacturing definitely has an effect on mechanical properties. However, the YS, UTS, and Young's Modulus value in Yiğitbaşı's research [19] is slightly higher. Although the manufacturing machine, process parameters, and material are the same, the dimensions and the shape of the specimens are different, and also the assumptions that were made during the tensile tests can be different because different test machines were used in the research [19].

1.2. Thesis Purpose

The fundamental topic of this study is to reveal both the static and dynamic mechanical properties of Ti6Al4V parts built by the EBM method and to analyze the manufacturing

direction effect on static and dynamic mechanical properties. According to the literature survey, the building direction affects E, YS, and UTS, and also Hardness (HRC) values. However, there is not enough research about the mechanical properties at high and ultra-high strain rates for the different building directions by using the EBM method. Therefore, the effect of building direction at high-strain rates and quasi-static processes is also evaluated in this study.

1.3. The Structure of the Thesis

In this study, the material properties, yield strengths, and endurance of the products are studied to provide suitable usage of AM Technology in the industry. The AM techniques, methods, and usage of these techniques according to the selected manufacturing technology are reviewed in the thesis. According to the manufacturing technique, the pros and cons and the working principle of each technique are specified. In addition, in this thesis, the EBM method is used in the static and dynamic mechanical properties of the Ti6Al4V and the properties are compared with the conventionally manufactured products' properties.

In the literature section, the basic information on the process technology that is used in additive manufacturing and its classifications are given. Along with these, the different methods that are used in the manufacturing of the products are explained and compared with the powder bed manufacturing technique.

In the results section, the results that are obtained within the purpose of the thesis, and the knowledge and gained experience are summarized. In this direction, the limitations and assumptions of the studies carried out for the thesis, the differences in evaluation caused or possible by these are presented, and the potential uses of the information obtained as a result of the thesis study are suggested. The possibilities of additional activities that will advance the thesis work are evaluated, and the thesis report is concluded with reference to future studies.

2. ADDITIVE MANUFACTURING TECHNIQUES

Additive Manufacturing method is described by international standards as a manufacturing method where designs are created from 3D data, by combining suitable materials according to design in layers stacked on top of each other [1]. Additive manufacturing technologies, which contain more detail than what is defined in the basic terminology standards, build parts in accordance with different principles. However, some process steps are common to the majority of different additive manufacturing technologies. Files that will control the additive manufacturing systems that are created during the work preparation stages, which start with the stereolithography (STL) file as a reference. The preparation of these files, which will control the additive manufacturing systems, starts with placing the part geometry on the building system. In the next stages, support structures are created under the protruding or overhanging surfaces. If it is desired to produce more than one of the geometries prepared in this way, reproduction is made and all the resulting geometries are divided into layers in the direction of the desired thickness. As a result of assigning process parameters, the production preparation phase is completed. At the last stage of the process, the finished piece is separated from the system that built it. The details of this stage also vary for different additive manufacturing methods. In the last case, secondary operations are performed on the separated part. Here, it is possible to benefit from many methods such as HIP, sandblasting, machining, polishing, and etching depending on the part material, geometry, and desired tolerances.

Parts with different purposes of use are manufactured with different methods developed by different companies. The most common of these methods are direct metal deposition (Direct Metal Deposition, DMD), electron beam melting (EBM), direct metal laser sintering (DMLS), electron beam free form fabrication (EBFFF), laser engineered net shaping (LENS), selective laser sintering (SLS) and selective laser melting (SLM).

2.1. Direct Metal Deposition (DMD)

The directed laser energy deposition process is known by the commercial application as DMD. In the process, the powder or wire is transferred to the environment by means of a guiding head, and in the meantime, the energy input is applied to the added material. In this way, the added material first melts and then solidifies and forms the relevant part of the piece. This process is repeated by means of a workbench with linear moving axes in a way to follow the units of the whole part geometry is completed. In this process, inert gas is used as a protective atmosphere [20].

This technology can be used to repair and rebuild damaged products and to produce new products and it provides anti-corrosive resistant coatings [20]. The working system are shown in Figure 2.1.

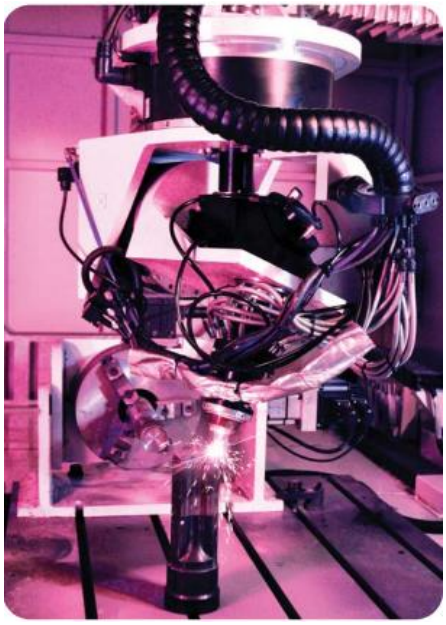

Figure 2.1: Direct metal deposition in action [20]

Direct metal deposition technology uses laser melting and a closed-loop system to provide dimensional accuracy [20]. The working system of DMD can be seen in Figure 2.2.

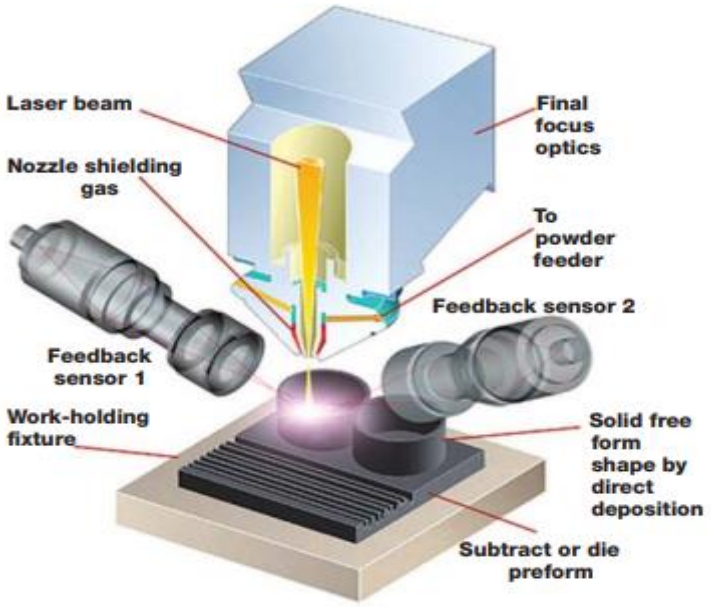

Figure 2.2: Schematic of DMD machine [20]

The Direct Metal Deposition closed loop system has an important role while manufacturing the products. It has high-speed feedback sensors to collect data about melting temperatures that directly control process inputs like laser power, dimensions, etc. (see Figure 2.2) [20].

The Direct Metal Deposition technology has been used for the manufacturing of gas turbine components, rebuilding tools like dies, cutters and remanufacturing, hard coating, and complex products in the industry. Besides, the heat input can be controlled during the direction metal deposition method so; parts can be manufactured with desired microstructures [20].

2.2. Electron Beam Melting (EBM)

The EBM method was made by ARCAM Company in Sweden. It is a method similar to DMLS technology as a solid pattern emerges from metal powders. The key difference is that in EBM the heat source is electron beams. EBM technology is a manufacturing method, which builds material layer by layer by melting completely dense metal powders with a powerful electron beam. The EBM technology has been successfully used in the medicine,

aerospace, defense, and automotive fields. It is a safe and environmentally friendly technology [21].

The usage of electron beam melting technology provides higher build rates by higher scanning velocities and higher penetration depths [21]. The basic working principle of laser beam-based technologies and electron beam melting technology is identical. The electron beam deflected the metal powder and processed the material powder thickness from 20 to 100 μm [21]. The working principle of the Electron Beam Melting process is shown in Figure 2.3.

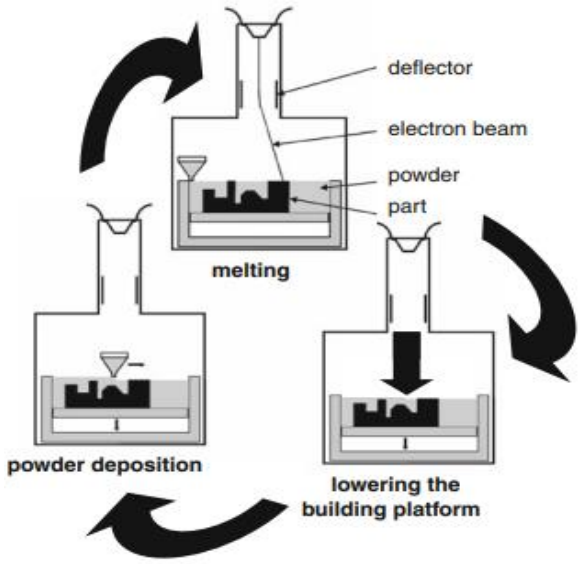

Figure 2.3: Working schmeatic of the EBM process [21]

The Electron Beam Melting technology has two critical processes namely melt ball formation and delamination. When the melt pool shows instabilities, the melt ball develops [21]. The melt ball occurs because of insufficient energy that is transferred from the electron beam into material powder. (See Figure 2.4)

Figure 2.4: Melt ball formation [21]

When the residual stresses occur in part surfaces, the delamination is observed. The delamination depends on scanning strategy especially energy inputs. (See Figure 2.5)

Figure 2.5: Delamination [21]

Finally, in Electron Beam Melting technology the scan speeds are smaller than in other technologies; however, it splits a single beam into multi-spots. Therefore, it is called multi-beam melting technology. This provides a reduction in production time due to the simultaneous melting facility [21].

2.3. Direct Metal Sintering (DMLS)

DMLS is an Additive Manufacturing method that use the method of spreading a metal powder and transferring them to the laser beam. The laser power, layer thickness, and

scan speed affect the mechanical properties of parts in DMLS technology [22]. The different mechanical properties of the product are adapted by calibrate the input parameters. Thus, the manufacturers do not need to make many trials on the machine [22]. The working principle of the Direct Metal Sintering method is shown in Figure 2.6.

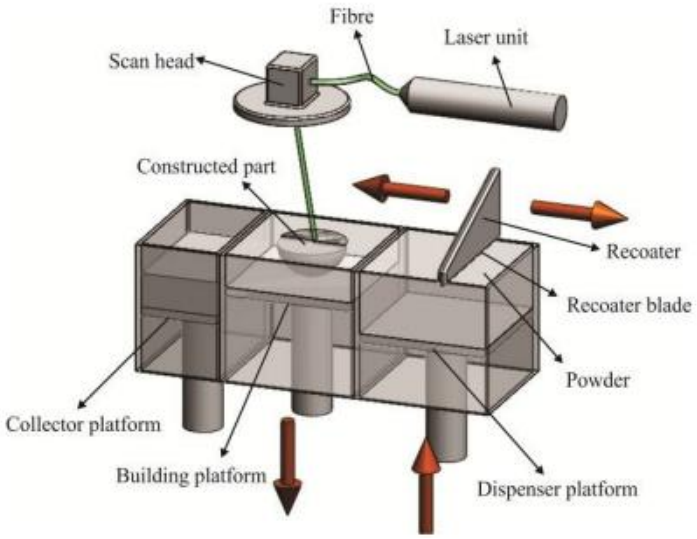

Figure 2.6: Schematic diagram of the DMLS system [22].

In DMLS technology, a thin layer material powder is spread. Then, the printing chamber of machine is heated. The laser processes the powder layer by layer and the part is sintered [22].

The most important advantage is DMLS parts do not need manufacturing tools like molds, manometers, etc. Therefore, initial part production time is reduced. In addition, additive technologies such as DMLS offers design customization and exchange by providing short-term ways and special products without incurring expensive tooling changes. The disadvantage of this technology is offering a lower dimensional area to manufacture parts compared to other technologies [23].

2.4. Electron Beam Free Form Fabrication (EBFFF)

EBFFF technology is one of the methods of additive manufacturing that uses advanced, complex manufacturing processes [24]. In the EBFFF process the deposition of metal occurs layer by layer by melting of wire. Then, the part obtains its net shape. The manufacturing process is shown in Figure 2.7.

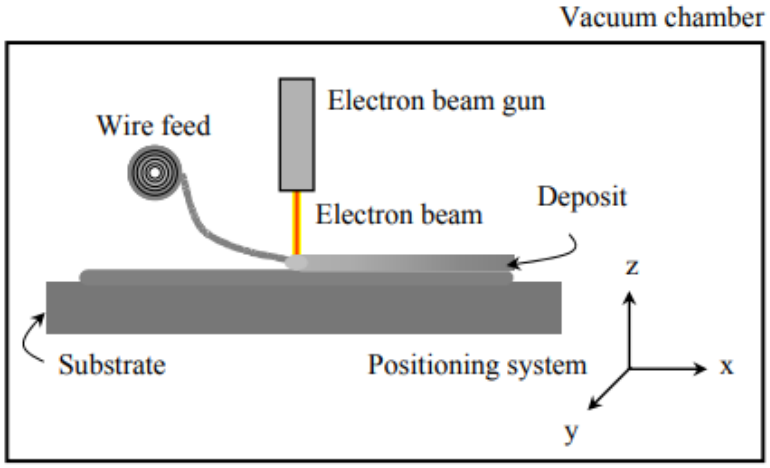

Figure 2.7: Schematic of EBFFF system [24]

The advantage of the EBFFF process is the deposition rate is higher than the other methods. It rates up to 12 kg/h. The other additive methods cannot reach this deposition rate value. In addition, this process allows fully dense and homogeneous products within 5000mm size [24].

The electron beam controls the voltage, current, distance and electron beam diameter, and scan speed [25]. The wire feed system consists of feed rate and table velocity with as regards the electron beam. In this process, the optimal values of these parameters are very crucial to obtain high-quality products. The feedstock diameter controls the smallest detail that is attainable in this process. The fine diameter controls the large details during bulk deposition [25].

The translation speed controls the dimensions of the powder layer and the higher translation speed provides cooling and results in a homogeneous microstructure like the one shown in Figure 2.8. However, the lower translation speed causes the inhomogeneous microstructure and larger grains [26].

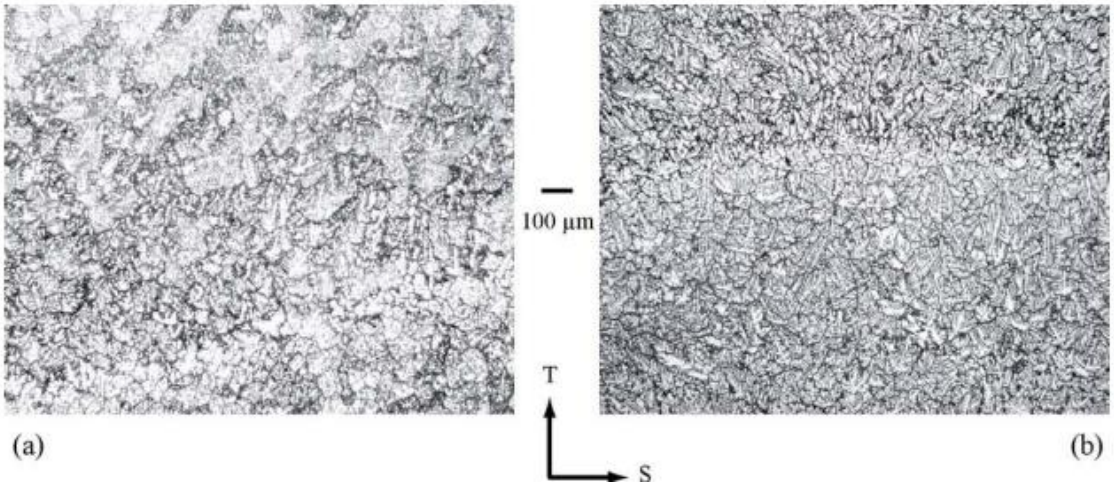

Figure 2.8: (a) Low Translation Speed inhomogeneous microstructure and larger grains (b) higher translation speed produces more homogeneous microstructure and smaller grains [26]

The Electron Beam Free Form Fabrication process can be used in the repair of products or parts that have bad tolerance. Moreover, the entire structure can be manufactured by this technology without any casting and forging processes. Thus, the process parameters such as deposition rates, efficiencies, material compatibilities, and qualities affect the entire manufacturing stages, and the raw material costs and manufacturing times can be adjusted according to input parameters [26].

The recent work with Electron Beam Free Form Fabrication is done by NASA Langley Research Center and it is stated that 2219 Al and Ti-Al6-4V materials can be used if the mechanical properties are optimized for this process because these materials have excellent weldability, strength, and toughness [26].

2.5. Laser Engineered Net Shaping (LENS)

LENS method is based on the principle that the powders sprayed from the nozzles are melted with the laser beam and knit side by side along the cross-section of the part in that layer. Metal powders are sprayed with the help of gas from the nozzles to the focal point of the laser where melting takes place. When the layer is finished, the table of the machine goes down one layer height, the new layer is knitted and the process is repeated until the part

is obtained. Parts obtained with LENS can be used directly as part of a machine. The method can also be used in some repair operations [27].

In the LENS system that is shown in Figure 2.9(a) melted the laser beam with scanning pulses and lines. It provides to produce high-quality products within control the dimensional accuracy. LENS system comprises a laser, lens, powder delivery nozzle, and adjustable laser head as can be seen in Figure 2.9(b). Unlike the powder bed systems, the energy and material deposition have occurred in the same region that controls the material feed. In addition, the laser beam can be moved in the Z direction; however, the platform remains fixed [27].

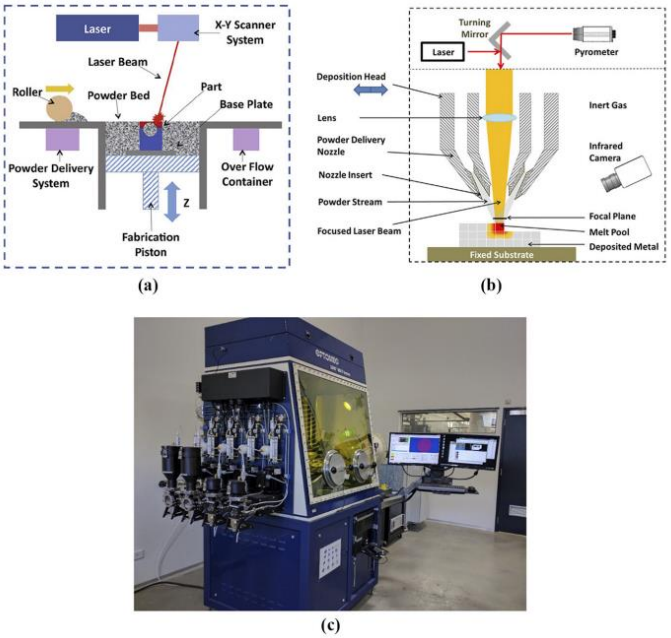

Figure 2.9: (a) Powder bed fusion schematically, (b) direct energy deposition (LENS)

(c) photograph of a LENS MR-7 [27]

Rapid prototyping methods are important manufacturing methods in which any part can be obtained without the need for a second process. LENS, one of these methods, gains more importance than the other methods because it provides ease of application and can be used as a functional part of a machine [27].

The most important advantage over other methods is that high-density parts can be obtained when the process parameters like speed, temperature, nozzle height, and powder amount are set to optimum values. Physical properties such as grain structure and surface quality can be very good. With the studies carried out, very important developments have been achieved in the method. [27].

2.6. Selective Laser Sintering (SLS)

SLS is one of the layered production techniques that make use of laser energy. In this method, the powder material is selectively sintered by a laser as a power source to form the part. It allows manufacturing of complex CAD products by metal/plastic powder technology [28]. The schematic process of Selective Laser Sintering technology can be seen in Figure 2.10.

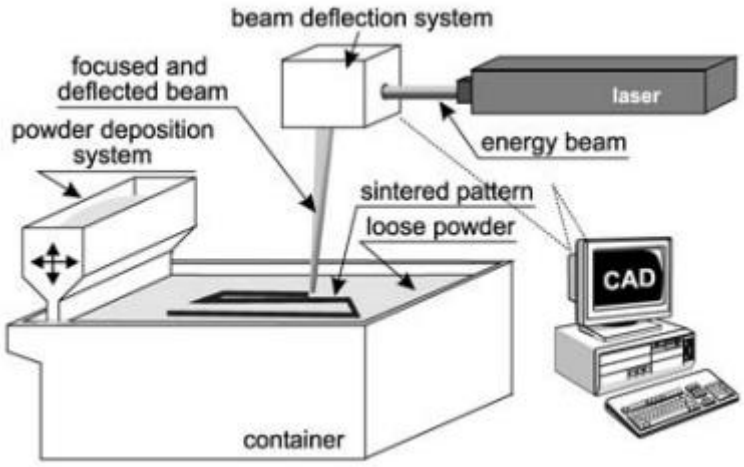

Figure 2.10: SLS Process Description [28]

In this system, alloy powder is piled up on a bed. With the help of a cylinder passing over the powder bed or a leveling system, a constant thickness of alloy powder is placed in the powder bed. Although the layer thickness of the material powder alloy layer is in the range of 20-100 μm in current technology, production with an average layer thickness of 0.1 mm is carried out. The galvanic mirrors located in the laser beam provide faster scan and sintering speeds for the production of the designed parts. This cycle continues until the production of the object is completed [28].

The support structures do not necessary in the manufacturing of parts in SLS method compared to other methods. However, in some polymer types, the need for a support structure may arise depending on the solidification rate or the design of the object to be produced. Only rough support structures can be used between the table and the object for positioning the object relative to the table.

After production, the free dust around or inside the part is removed manually with the help of a brush or vacuum suction after production. Since it has a rigid structure, it does not need an additional process such as curing. Only metal parts can be annealed to increase the strength of the part. The part should be left to cool after the production is finished [29].

In the Selective Laser Sintering method, parameters such as scan speed, powder properties, pulse frequencies, laser power, scan properties, bed temperature, layer thickness, and the ratio of powder mixture are also important in production. In addition, fabric orientation and packing affect the optimization of the SLM machine [29]. The SLM process description is shown in Figure 2.11.

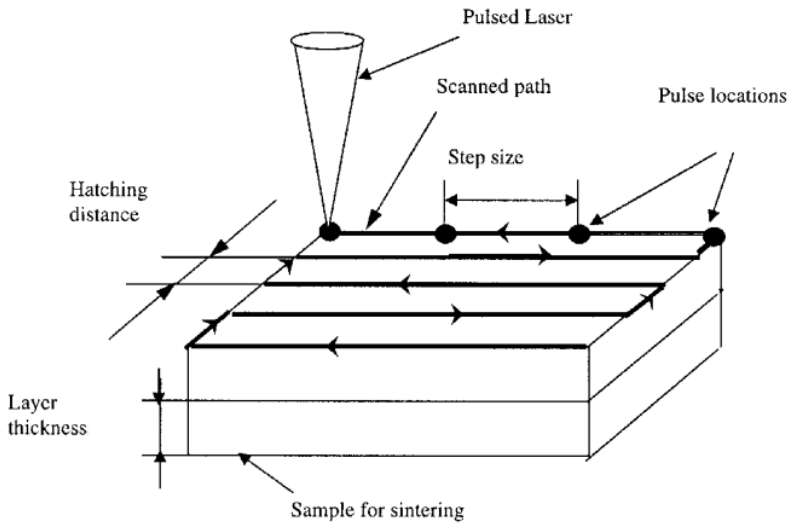

Figure 2.11: SLS System Description [29]

The advantages of the SLS method can be stated as [29]:

- It is possible to manufacture metal parts with SLS,
- Parts having complex geometries that are very difficult to produce with traditional methods, parts can be produced.
- Precision production of detailed designs can be realized.
- The quality of the surface of the part is high depending on the layer thickness.
- High-strength parts can be produced.
- Production can be carried out without the need for support structures.
- Post-production labor is less than other methods within the SLS method.

The disadvantages of the SLS method may be given as;

- Machines working with the SLS method are expensive.
- Compared to other production methods, the manufacturing cost (material, depreciation, time, etc.) is higher.
- It is not suitable for mass production in current technology.
- There is a need to apply the final treatment (heat treatment, sandblasting, etc.) to the manufactured parts.
- Depending on the part, it may take a certain period of time for the part to cool down after manufacturing [29].

The desired properties of the products can be obtained by changing the material properties and process parameters and then, the process will be optimized to manufacture high-quality products [29].

2.7. Selective Laser Melting (SLM)

SLM is an additive manufacturing method in which a laser is used to melt and process the metallic powders. [30]. The Selective Laser Melting process can be seen in Figure 2.12.

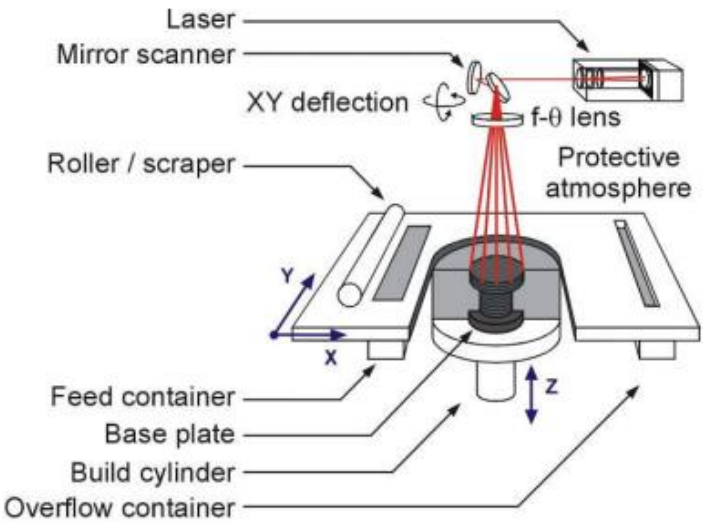

Figure 2.12: SLM Process Description [30]

This advance is crucial for material industry, as it can not only create special design properties but also reduce material excess and provide more facility with designs that other techniques cannot provide [30]. Demands such as the need in fabrication material and special applications that require complex products are common challenges in the industry. SLM not only improves the process of creating and selling. The challenges with SLM are to have a limit on materials, process parameters, and microstructural defects like crack and porosity [30].

The difficulties are the inability to form 100% dense parts due to difficulties to use metal powders. Aluminum powders are light and have high reflectivity, thermal conductivity, and low laser absorption for the lasers used in SLM. These challenges need to be developed by further studies [30].

The mechanical properties of metal alloys manufactured by SLM can diverge significantly from its conventionally manufactured parts. The metal alloy strength produced by SLM tends to be significantly poor then pure metals. The decrease in mechanical properties of the manufactured parts is based on the defects and porosities in microstructure occurred in the SLM process [30].

A central feature of alloys produced with SLM is that the product may show great anisotropy in mechanical properties. The grain size in cast metals is featured by uniform, isotropic grains, while metal alloys show great grain elongation in the direction of the structure. Anisotropy in grain size is interrelated with anisotropy of surface defects, crack propagation direction, and mechanical properties, and there are significant decrease in hardness, strength, and ductility under tension [30].

For the time being the industrial applications of the SLM is given below [30].

- **Aerospace**: Air ducts, fixtures, or complex structural assemblies for equipment.
- **Manufacturing:** Low-volume markets at competitive costs. Independent from economies of scale and focus on optimization of products.
- **Medical**: For complex, expensive and high-value medical devices.
- **Prototyping**: Laser sintering can provide manufacturing the demanded design and functional prototypes. As a result, the operational tests can be done according to the design.
- **Tool Machining:** Direct machining eliminates tool need for production and various machining operations.

The SLM technique is used to produce prototypes and build up final products. Some of the current applications of Selective Laser Melting can be seen in Figure 2.13.

Figure 2.13: Current applications of SLM [30]

The design limits are important in SLM technology because the surface finish process and the layer thickness result in the staircase effect after manufacturing. This causes a raise

in the surface roughness and resistance of parts [31]. The CAD geometry shows the internal gussets to overhang features, trusses with hollow elements, and bulkheads to provide endurance and also reinforcement to prevent local buckling [31]. The optimized geometry example of CAD can be seen in Figure 2.14.

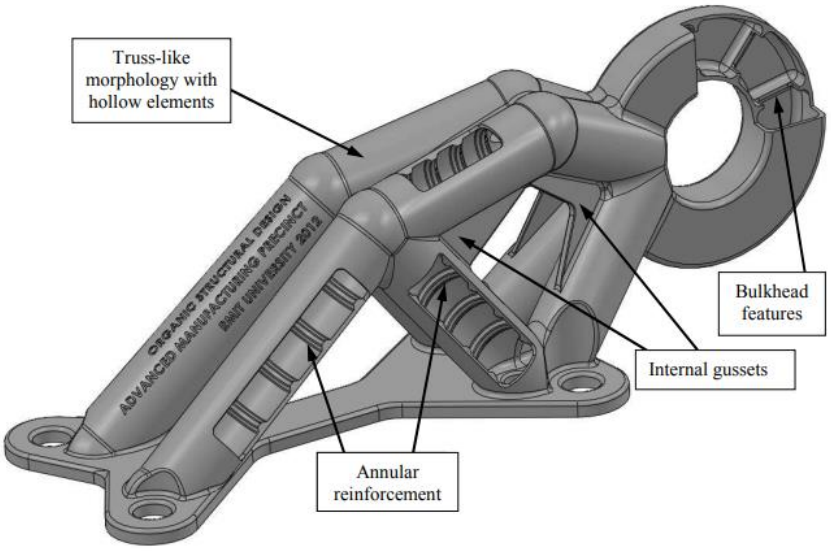

Figure 2.14: Parametric optimization geometry. Cutaways included Internal features [31].

The optimization process can be monitored to provide quality assurance for closed-loop feedback control systems [32]. The SLM is a useful method for complex products from metals and their alloys. The mechanical properties of materials are affected the strength and plasticity of the layer thickness during manufacturing [33]. This technology is used globally in industrial areas because of its benefits that offer ease of component design, short production times, and manufacturability and it replaces the traditional manufacturing technologies thanks to designed products and productivity with optimizing the suitable laser powers for demanded design [33].

2.8. Metals in Additive Manufacturing

Additive manufacturing technology is rapidly evolving. The additive manufacturing materials provide a summary of the processes of manufacturing [34]. The metals, graded alloys, and refractory alloys are searched for understanding the outputs of the additive manufacturing technology [34].

The materials that are used in AM, their processes, structure, and the mechanical properties of manufactured metals are explained in section 2.8. The Designing rules and stages are explained in section 2.9.

Additive manufacturing technology uses materials such as powder, wire, or sheets by melting and solidification with the laser, electron beam, or ultrasonic vibration according to processes that are selected by the manufacturer [34]. The specific AM alloys and their application area are indicated in Table 2.1.

Table 2.1:Common additive manufacturing alloys and applications [34].

Alloys Applications	Aluminum	Maraging Steel	Stainless Steel	Titanium	Cobalt chrome	Nickel Super Alloys	Precious metals
Aerospace	X		X	X	X	X	
Medical			X	X	X		X
Energy, oil and gas	X		X				
Automotive			X	X			
Marine			X	X		X	
Machinability and weldability	X		X	X		X	
Corrosion Resistance			X	X	X	X	
High Temperature			X	X		X	
Tools and molds		X	X				
Consumer Products	X		X				X

The DED and powder bed fusion technologies are compared in Table 2.2. The additive manufacturing process is selected according to the product that has desired size, quality, and complexity. The alloy powder-based processes are used to fabricate complex products with a higher surface finish. However, this process is slow and the feedstock of powder is expensive. Otherwise, the additive manufacturing processes that are wire and metallic sheet technologies are fast but lack dimensional quality and causes poor surface quality [34].

Table 2.2: Comparison of two main categories of additive manufacturing processes for metallic components: directed energy deposition (DED) versus powder bed fusion (PBF) [34].

Process	DED	DED Wire	DED Wire	Powder (PBF)
Feedstock	Powder			
Heat source	Laser	E-beam	Electric arc	Laser / E-beam
Power (W)	100-3000	500-2000	1000-3000	50-1000
Speed (mm/s)	5-20	1-10	5-15	10-1000
Max. feed rate (g/s)	0.1-1.0	0.1-2.0	0.2-2.8	-
Max. build size (mm x mm x mm)	2000x1500x 750	2000x1500x750	5000x3000x1000	500x280x320
Production time	High	Medium	Low	High
Dimensional accuracy (mm)	0.5-1.0	1.0-1.5	Intricate features are not possible	0.04-0.2
Surface roughness (µm)	4-10	8-15	Needs machining	7-20
Post processing	HIP and surface grinding are seldom required	Surface grinding and machining is required to achieve better finish	Machining is essential to produce final parts	HIP is rarely required to reduce porosity
References	[35], [36]	[37], [38]	[39], [40]	[41], [42]

Steel is the most common material that is used in industry so, it is also commonly used in additive manufacturing technology. The AISI 316L, AISI 304L, maraging steel 18Ni-300, and stainless steels 17-4 and 15-5 are used in Laser Based Methods [34]. However, the Electron Beam Based methods are mainly used steel H11, H13, and stainless steel 316L. The material selection also depends on the application and method of design.

Aluminum alloys are also used in Additive Manufacturing technology because Aluminum is easy to machine and the price is lower than other metals. However, manufacturing aluminum is also harder because it is hardly weldable. In addition, Aluminum alloys become stronger after precipitation hardening [34]. The most common Aluminum alloys that are used in Additive Manufacturing technology are AlSi10Mg and AlSi12. In locations that need high-strength properties Al-Mg-Sc alloy can be used in these areas [34].

Titanium and its alloys are also used in Additive Manufacturing technology. It provides high performance, and also lower production costs and production times with

respect to conventional production methods. Therefore, additive manufacturing technology provides cost and time advantages for Titanium alloys [34]. The Ti6Al4V is the most common material used in the production of parts despite the fact that it is still being investigated for industry [34]. Ti6Al4V titanium alloys are used in the Laser Based and Electron Based Methods because of the great allotropy of Titanium [34].

Other than Steel, Aluminum, and Titanium alloys, Nickel based alloys are also used in Laser Based and Electron Based Methods for biomedical applications [34].

The various materials that are used in different additive manufacturing techniques are shown in Figure 2.15. The Laser based techniques like SLS, SLM, DMLS, DMD, LENS, SLC, and electron beam melting (EBM) use powder bulk material type. The Material jetting techniques use Liquid bulk material type. However, Extrusion Thermal and adhesion techniques use solid bulk material types [44].

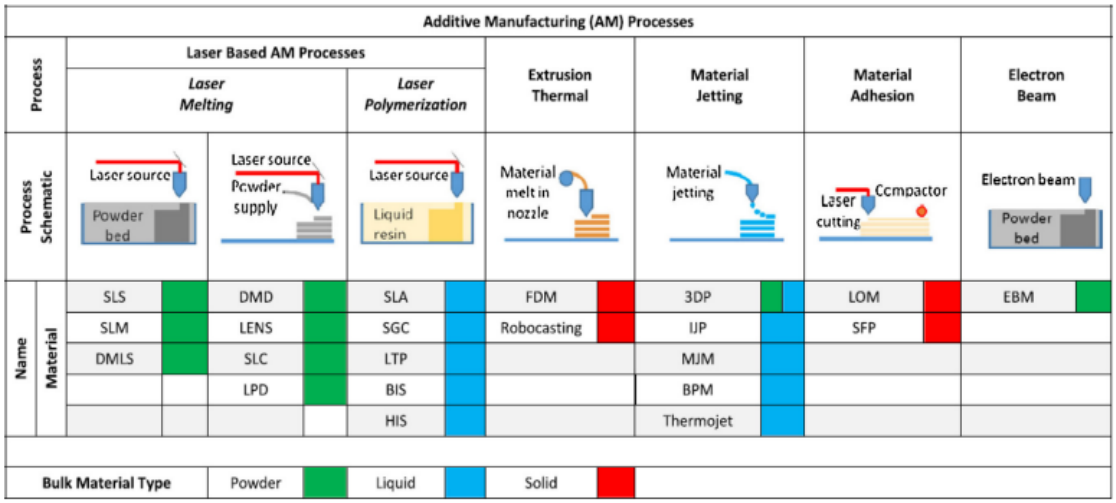

Figure 2.15: Materials category for AM technologies [44].

Additive manufacturing is not only used in the aerospace, and transport industries, it is also used in the medical industry because the metals have been used in the medical industry for more than 120 years ago. Titanium, cobalt, alumina and zirconium are most processed materials in the medical industry. The list of the materials and the application areas are specified in Table 2.3 [44].

Table 2.3: Biomedical materials [44].

Implant material	Abbreviation/notation	Application
Ti and Ti alloys	CP–Ti	Bone fixation
	Ti–6A1–4V	Artificial valve, stent, bone fixation
	Ti–6Al–7Nb	Dental application, knee joint, hip joint
	Ti–5Al–2.5Fe	Spinal implant
	Ti–15 Zr–4Nb–2Ta–0.2Pd	Dental applications
	Ti–29Nb–13Ta–4.6Zr	Dental applications
	83%–87%Ti–13%–17%Zr (Roxolid)	Dental application
Stainless steel	316L	Dental, knee joint, hip joint, surgical tools
Cobalt chromium alloy	Co–Cr–Mo, Co–Ni–Cr–Mo	Artificial valve, bone fixation, dental applications, knee joint, hip joint
Shape memory alloy	NiTi	Catheters, stents
Polymers	PMMA, PE, PEEK	Dental applications, articular cartilage, hip joint bearing surface, knee joint bearing surface, soft tissues
Bio-glass	$SiO_2/CaO/Na_2O/P_2O_5$	Dental applications, orthopaedic implants
Zirconia	Zirconia	Porous implants, dental applications
Alumina	Al_2O_3	Dental applications
Hydroxyapatite	$Ca_5(PO_4)_3(OH)$	Dental applications, implant coating material

The materials that are used in additive manufacturing technology have been explored to provide high-quality products according to additive manufacturing techniques. The developments of new materials provide new innovations in this area and provide a way to study new production methods according to the technique that is used in additive manufacturing [44]. After the trials, the mechanical properties of the alternative materials can be understood and lots of development will be done in additive manufacturing and the material industry.

2.9. Designing for Additive Manufacturing

AM technologies are employed for producing 3D products by adding the selected material in machine table layer by layer. The manufacturing process needs design guidelines and principles to design and manufacture high-quality parts [45]. The design process can be handled under four stages such as task explanation, conceptual design, embodiment design, and final design [46, 49]. Each stage requires a different guideline to show a pathway to designers. The design guideline is also handled under three stages that are process characteristics, design principles and rules. The design guidelines are primarily focused on the AM processes, especially for SLS, SLM, and FDM [45]. A flow chart for designing a part is indicated in Figure 2.16.

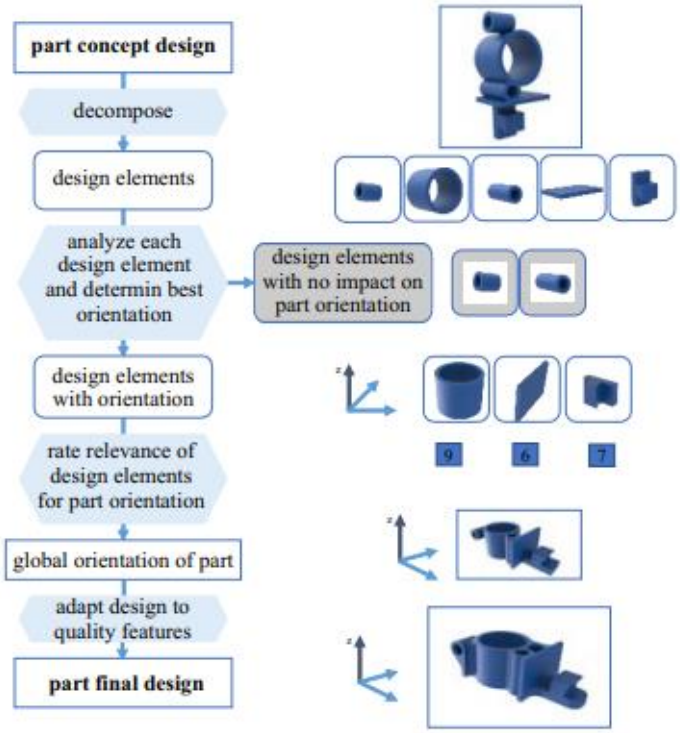

Figure 2.16: A flow chart for design stages [45].

2.9.1. Process Characteristics

The working principle of the manufacturing process for a designer to design proper parts by using Additive Manufacturing technology is summarized in the process characteristic stage. The process characteristics have an impact on the design and also on parts which are manufactured by additive manufacturing [48]. The different process features of different Additive Manufacturing techniques can be taken from literature studies [48, 49].

2.9.2. Design Principles

The design principal stage is one of the important stages for additive manufacturing designing because the design principle provides designers to turn their things into the optimum design by reducing the manufacturing costs and increasing the part qualities. In this stage, the designer has to learn the design principles of both conventional manufacturing and additive manufacturing methods. Therefore, a designer can select which method is suitable for the design to produce high-quality parts [45].

2.9.3. Design Rules

The design rules consist of design characteristics and principles for a designer to design producible parts for the AM process. The design rules are composed according to the material of the part, the process, and also machine parameters. The initial machine parameters can be taken from the similar researches; however, the design characteristic parameters need to be chosen by the system that the designer is using. The design rules also cover wall thickness values and roughness information that can be changed with process parameters [45].

2.9.4. Part Orientation

In the AM process, the building direction and part geometry are crucial to manufacturing high-quality parts. The manufacturing orientation indicates the build direction of the part around the build axes during manufacturing [50]. The Additive Manufacturing process requires support structures in the build direction to manufacturing complex shapes. Therefore, the part orientation is significant in the design of demanded product [50]. For example, the inner radiuses of a curved element need to be designed according to design rules to provide part orientation during manufacturing [45]. The Part Orientation percentage of SLM, SLS, and FDM are shown in Figure 2.17.

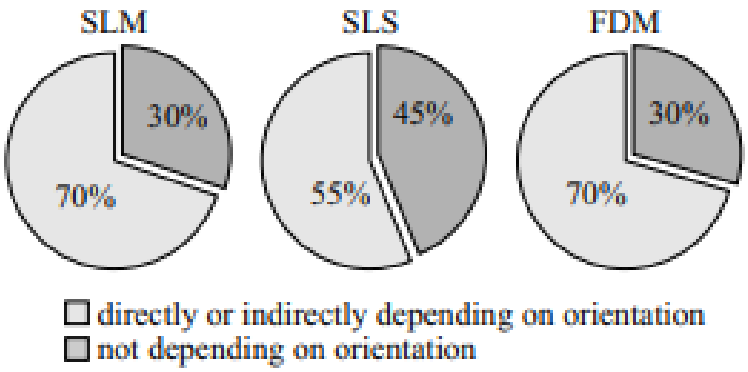

Figure 2.17: Part Orientation percentage of AM methods [45].

The part orientation is built upon different quality features such as dimensional and design accuracy and surface smoothness, manufacturing costs and time etc. [51]. These properties are dependent on the design geometry. After the final design of the part, the part is rotated according to part orientation to achieve optimum quality. The result of this optimization provides a balance in different quality features [52].

2.9.5. Manufacturing Constraints

There are two different constraints for additive manufacturing technology in the literature. The first main constraint is the nozzle position. The nozzle has to located parallel to the table axis and the product needs to be mounted on a rotating platter. The second main constraint is the acceleration levels of the nozzle during the depositing of the material. The repetition causes the stop of the manufacturing because of molten drops solidify. To avoid this repetition, the design needs to be optimized by increasing the corner smoothness and giving them a radius [53].

The powder usage at high temperatures can cause defects and porosities and poor mechanical properties. Therefore, researches are conducted to finalize the usage of additive manufacturing technology with other metal alloys. The results of these experiments are also used in FEM analysis of the manufactured parts [53].

2.9.6. Manufacturing Capabilities

Additive manufacturing technology has the ability to manufacture complex geometrical shapes by using different manufacturing principles. The scanning processes for the manufacturing are given the design of part while the nozzle is still parallel to the manufacturing surface [53]. In addition, the material is used according to the demand contrary to the conventional manufacturing methods. The lattice structures can be used if the parts need to be dense and rigid [54].

In the layer-based processes, the manufacturing starts at the plane surface, then the material is deposited to substrate the complex surfaces. This capability provides multi-functionality since different processes can be worked at the same time such as remanufacturing or repairing the parts [53].

The additive manufacturing technology decreases the price between different metallic alloys such as titanium and aluminum because of the greater mechanical properties and lower densities. Therefore, the designers can select the materials without any doubt. In addition, additive manufacturing technology has the capability to produce new materials that are reproduced by steel, aluminum, etc. [55].

2.9.7. Parametric Optimization

While designing a product for additive manufacturing technology, the manufacturing time, raw materials, energy consumption, and manufacturing costs are related to the production and design of the part. To minimize the part size optimizing for AM can be done [54]. An example of CAD design that is manufactured on an EBM machine with titanium alloy Ti6Al4V is shown in Figure 2.18.

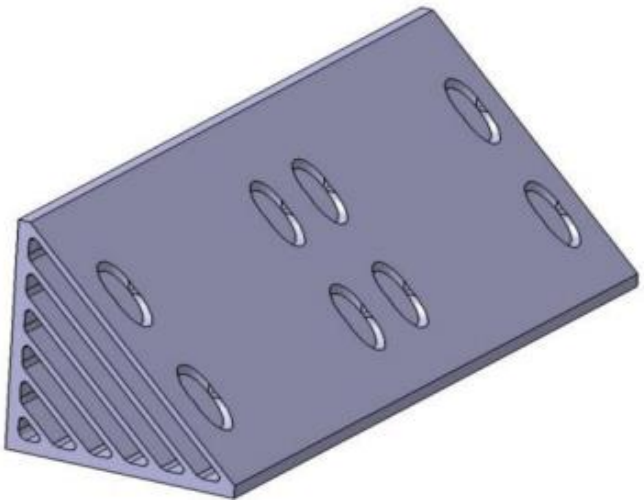

Figure 2.18: Example of new design manufactured in Ti6Al4V on EBM machine [54].

The main aim of the optimization stage is to minimize the size of the part by optimizing the boundaries and process parameters. The optimization can be done by using modeling and simulations to obtain stiff parts. For the simulations, the finite element analysis will be conducted to indicate parts boundaries when it is loaded. However, when parts are manufactured by additive manufacturing technology, parts contain complex lattice

structures, so the finite element analysis cannot indicate the real results because the number of parameters is high [54].

3. MATERIAL AND METHOD SELECTION

The thesis study is conducted to determine the usability of Additive Manufacturing technology in the aerospace industry. The properties of Ti6Al4V are determined by the transformation of the alpha and beta phases. In industrial applications, Titanium alloys are selected according to the transformations of the phases, and phases close to α/β and β are often recommended in biomaterial manufacturing. Ti6Al4V is frequently seen in the literature as the material of choice for aircraft landing gear, gas turbine wheels, and implant manufacturing. However, after the production of these alloys by casting method, the use of machining processes leads to high costs with material consumption, along with machining difficulties. Therefore, the production of parts from these expensive alloys necessitated the use of parts production techniques close to the final shape.

3.1. Material Selection

Ti6Al4V titanium alloy is widely used in aerospace and medical industries because of its good mechanical properties, low density, and good machinability [56]. The Ti6Al4V titanium alloy can be manufactured by using conventional methods like casting, forging, and machining. This metal is most widely used in high-performance applications where products are exposed to cyclic loading and fatigue cycles [57]. The studies indicate that the EBM and SLS technologies provide lower surface roughness value but higher fatigue life. However, still, additive manufacturing technology is improving in terms of fatigue life but the parts produced still have lower fatigue life than the parts manufactured by conventional methods [58]. Metal-based additive manufacturing technology, which has been developed recently and uses laser-assisted Ti6Al4V powders, has been embraced by the aerospace industry. In addition to being used in the fuselage of airplanes, engine companies manufacture complex parts with this method [58]. In this thesis, Ti6Al4V Powder of GE Company that is used for manufacturing of test specimens is shown in Figure 3.1.

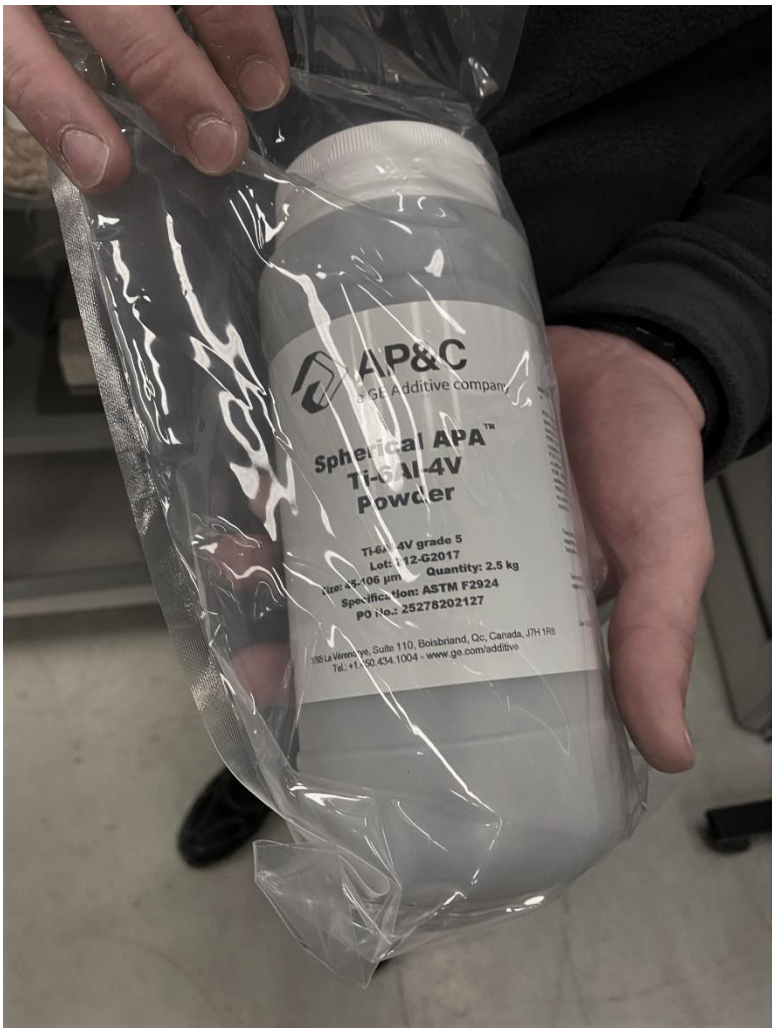

Figure 3.1: The Ti6Al4V Powder used in manufacturing

When the studies on the Ti6Al4V titanium alloy were examined, it was seen that the Ti6Al4V titanium alloy is among the hard-working alloy and causes rapid wear of the tool and poor machined surface quality [58].

In order to overcome these deficiencies, the following points should be considered.

- Since the cutting speed increases the processing temperature, it should be chosen at the lowest value according to the catalog value of the cutting tool.
- Since the feed causes high deflection, vibration, and cutting force, it should be chosen very low.
- In milling and turning operations, the depth of cut should be low.
- Cutting tools with high wear resistance and chemical stability should be used.

- Pressurized coolants with lubricating properties should be preferred.

The mechanical properties of the Ti6Al4V Powder of GE Company are indicated in Table 3.1.

Table 3.1: Mechanical Properties of Ti6Al4V Powder of GE Company [58]

Mechanical Properties	Metric	English
Hardness, Rockwell C	33	33
Tensile Strength, Yield	**951 MPa**	**138000 psi**
Tensile Strength, Ultimate	1020 MPa	148000 psi
Elongation at Break	**14 %**	**14 %**
Reduction of Area	40 %	40 %
Modulus of Elasticity	**120 GPa**	**17400 ksi**
Fatigue Strength	600 MPa	87000 ksi
Density	**4.43 g/cc**	**0.160 lb/in**

3.2. Mechanical Modelling and Manufacturing Method

3.2.1. Specimen Dimensions in Quasi-Static Tests

In the thesis, the ASTM E8 standard was taken as a reference for the quasi-static mechanical tests. As with other test methods, the sample has to be suitable for the test and in ideal dimensions. In the scope of this thesis, rectangular specimens Ti-6Al-4V are manufactured for mechanical tests.

The thickness, width, and length dimensions of the samples have restrictions followed by a reference to the ASTM E8 standards as follows:

- In order to minimize the margin of error in the calculation of the shear modulus, the width/thickness ratio must be greater than 5.
- All surfaces of the produced rectangular samples must be flat. Parallelism of opposite surfaces along the length, width, and thickness of the sample rate should be within 0.1%.
- The length of the sample should be measured with a maximum difference of 0.1% thickness and width and a maximum 0.1% difference in measurements to be made from 3 different points is required.

- There should be no large cracks or small cracks and defects on the specimen surface and interior of parts that will be tested.

3.2.2. Material and Powder Characteristics

The specimens that are produced by Ti6Al4V titanium alloy are manufactured with ARCAM Q20 plus machine shown in in Figure 3.2.

Figure 3.2: Arcam Q20 Plus [58]

The Ti6Al4V grade 5 powder is used for specimen manufacturing and the dimensions of the powder is around 45-106 μm. The chemical property of the powder is given in Table 3.2.

Table 3.2: Chemical Properties of Ti6Al4V Grade 5 Powder of GE Company [58]

Titanium	**Balanced**
Aluminum	6%
Vanadium	4%
Carbon	0.03%
Iron	0.1%
Oxygen	0.15%
Nitrogen	0.01%
Hydrogen	0.001%

All samples are produced with the same production parameters within the scope of the thesis. Production parameters that are recommended and implemented by ARCAM Company are shown in Table 3.3, Table 3.4 and Table 3.5. To summarize the definitions of production parameters: Layer thickness is one of the main production parameters and depends on the size of the powder material. This parameter directly affects the quality of the produced geometry.

3.2.3. Process Parameters

The beam current parameter is associated with the energy input of the manufacturing process. The choice of this current depends on the geometry of the sample that is produced. Low current ratings are used for thin parts, while high current ratings are used for large parts. The focal offset is the offset from the zero position to the focal plane. Increasing the focal offset decreases the energy density and melting depth. Thanks to the preheating temperature, while the layers are being produced, the dust particles are easily sent away with the high energy produced by the beam. This temperature is close to the main melting temperature.

Table 3.3: Pre-heating Parameters of ARCAM Q20 Plus

Focus Offset	**44 mA**	
Melting Focus Offset	100 mA	
Max. Heating Time	60 s	
Square Dimension	144 mm	
Part Offset	4 mm	
Maximum Current	48 mA	
Pre- Heating Process 1 / Pre- Heating Process 2	**Max. Beam Current**	36 mA / 45 mA
	Min. Beam Current	36 mA / 45 mA
	Beam Speed	40500 mm/s / 40500 mm/s
	Repetition Number	3 / 3
	Line Offset	0.4 mm / 0.4 mm
	Scanning Depth	0.09 mm / 0.09 mm

Table 3.4: Melting Parameters of ARCAM Q20 Plus

Melting	Surface Temperature	**925 °C**		
	Maximum Depth	65 mm		
	Contours	**Contour Number**	3	
		Outer Contour / Inner Contour	**Bundle Speed**	450 mm/s / 450 mm/s
			Max. Bundle Current	9 mA / 9 mA
			Offset	0.27 mm / 0.18 mm
			Focus Offset	6 mA / 6 mA
	Scanning	**Max. Beam Current**	28 mA	
		Line Offset	0.22 mm	
		Scanning Depth	0.9 mm	
		Min. Current	3.5 mA	
		Scanning Length	45 mm	

Table 3.5: Support Structure Parameters of ARCAM Q20 Plus

Current	**10 mA**
Speed	1950 mm/s
Focus Offset	9 mA

3.2.4. Specimen Orientations

As a result of the literature review, the samples of the same size produced in different construction directions by the EBM method that was placed on the same table can show different mechanical properties [58]. Within the scope of this thesis, in order to examine the mechanical effects of the building direction of specimens, two different construction directions were chosen vertical and horizontal. Five samples were produced for each orientation as shown in Figure 3.3.

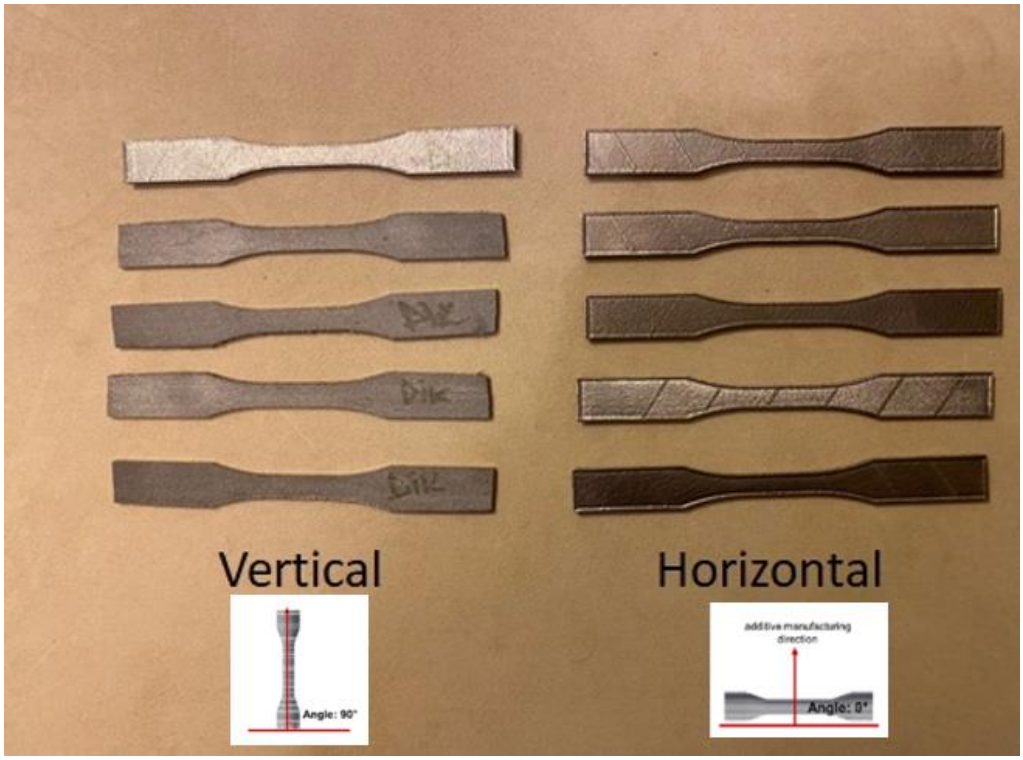

Figure 3.3: Samples manufactured in different building directions

The support structure was used because the surface area of the samples produced in the horizontal construction direction was too large to be built layer by layer. These support structures prevent distortions that occur due to thermal expansion during production. The support structure helps to dissipate heat. The support structure of the horizontal samples can be seen in Figure 3.4 and Figure 3.5.

Figure 3.4: Horizontal Sample Side Support Structure

Figure 3.5: Horizontal Sample Lower Support Structure

The static and dynamic mechanical properties of the manufactured specimens are affected by the position of these samples on the table during production. The cooling rates of the samples at different positions on the table are different. This is due to the fact that samples of the same size are produced with different cooling rates.

The manufactured samples need certain cleaning processes after manufacturing. This cleaning process varies according to the dimensions of the produced parts. The roughness is too high on the surfaces where the samples produced in the horizontal direction come into

contact with the table can be seen in Figure 3.6. Therefore, the surfaces need to be processed before the mechanical tests.

Figure 3.6: Sample Surface Roughness after Manufacturing

After manufacturing the parts, the surface needs a surface finish because of the support structure removal. The sandblasting process was carried out to minimize surface defects and support structure remnants. The process can be seen in Figure 3.7.

Figure 3.7: Sandblasting of Manufactured Part

After the sandblasting process, the parts are located in sanding machine for stoning. In the stoning process, the surface remnants were removed and the surface finishes were optimized for demanded value.

4. EXPERIMENTAL STUDY AND RESULTS

Three in horizontal and three in vertical building directions, a total the six samples were produced by ARCAM Q20 Plus Additive Manufacturing Machine. During the process, all of the manufacturing parameters were not changed except the building direction. The support remnants and surface remnants were removed by using sandblasting and grinding methods because the remnants decrease the both static and dynamic properties of the specimens. The quasi-static tensile tests and hardness tests were performed on the manufactured specimens to examine manufacturing direction effect on mechanical properties.

4.1. Density Measurements

The Ti6Al4V grade 5 powder is used for specimen manufacturing and the dimensions of the specimens is around 45-106 µm. The particle size and Volume graph is given in Figure 4.1.

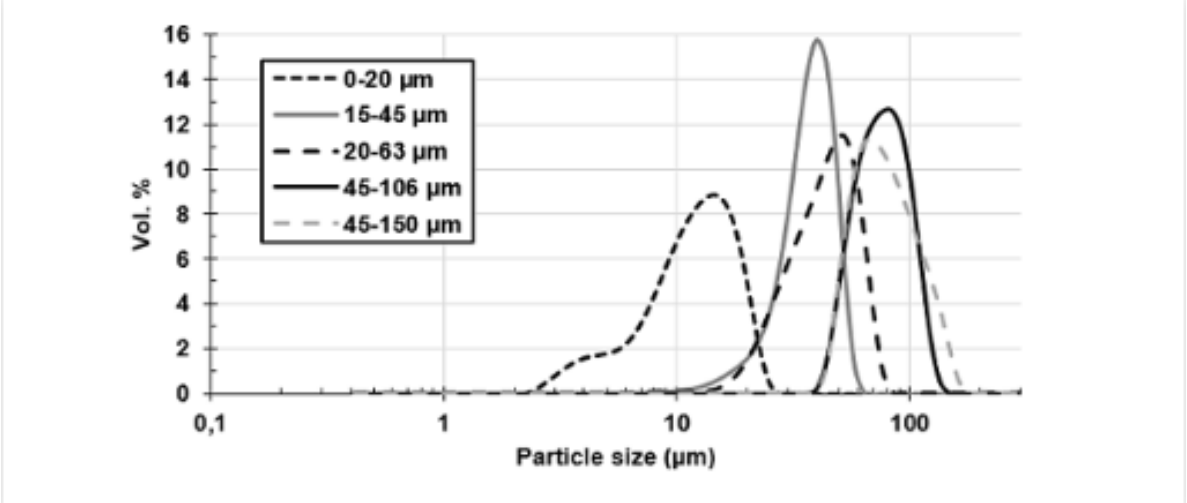

Figure 4.1: GE Company Ti-6AI-4V Grade 5 Particle Size and Volume Graph [59]

After sandblasting and stoning of the specimens, the density was measured by Archimedes Density formula. The density was measured with pure water (H_20) with 1.0 gr/cm^3 by scales. Before the measurement, the temperature of the pure water was measured, and then the weight of the specimen was measured in air. In addition, the weight of the specimen was measured in pure water. Then, the results were used in equation 4.1.

$$\rho = \frac{m_a}{m_a - m_b}(\rho_0 - \rho_L) + \rho_L \quad (4.1)$$

where,
ρ = Specimen Density
m_a= Specimen weight in air
m_b= Specimen weight in pure water
ρ_0 = Density of pure water (1.0 gr/cm^3)
ρ_L = Density of air (0.001223 kg/m³)

The densities were calculated both the vertically and horizontally manufactured specimens. The Powder (Ti-6Al-4V Grade 5) and specimen densities are shown in Table 4.1.

Table 4.1: Density comparison of Ti6Al4V and Specimens

Specimen	Density (g/cc)
Ti-6Al-4V Grade 5	4.43
Y (Z-direction)	4.39 (99.2%)
D (X-direction)	4.40 (99.4%)

There is 0.6-0.8% density difference between Ti6Al4V Grade 5 Powder density value and the manufactured specimens. This difference occurs comes because of the manufacturing method. In the additive manufacturing method, some porosities occur in the microstructure. Therefore, the density values change according to the manufacturing properties and methods and manufacturing direction.

4.2. Surface Roughness Test of Specimens

For surface roughness measurements, Mahr Marsurf GD25 that is shown in Figure 4.2 was used. The rotary probe is adjusted according to the manufacturing plane with respect to the specimens' surface. A complete revolution causes an inclination modification of 6 µm/mm; one scale division corresponds to an inclination modification of 0.1 µm/mm.

Figure 4.2: Mahr Marsurf GD25 Surface Roughness Test

The surface roughness measurements were taken from three different locations on each specimen. The measurement direction is selected as perpendicular to its horizontal length linearly and the average surface roughness values Ra are measured via a computer program that is connected to the tester. The measurement directions (1, 2, and 3) are shown in Figure 4.3.

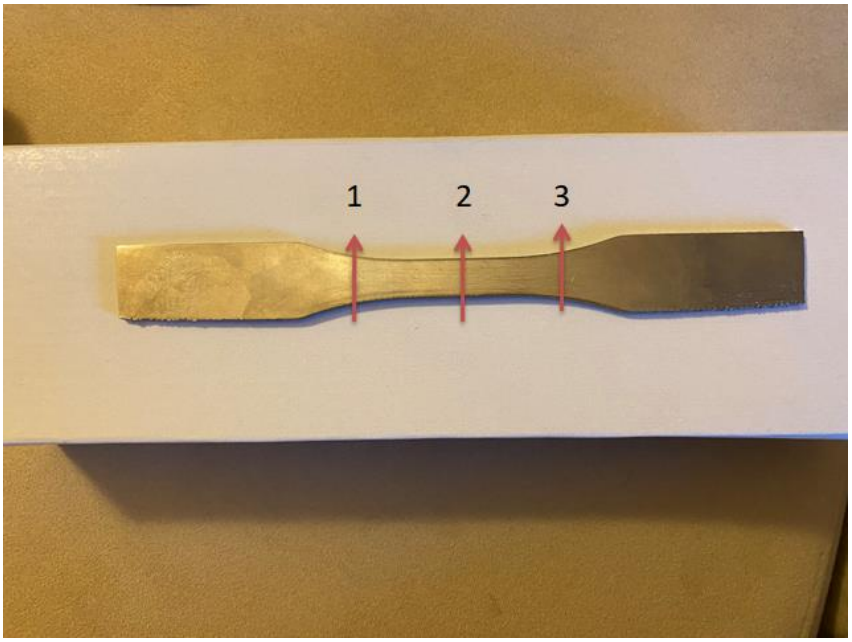

Figure 4.3: Surface Roughness Measurement Directions

During the measurement, the three measurements were done between the gauge length of the specimens. The vertically (Y specimens) manufactured specimens have higher mean surface roughness values compared to horizontally (D specimens) manufactured specimens. The results of the surface roughness measurement are shown in Table 4.2. The D specimens have lower surface roughness; therefore, the elongation rate that is shown in Table 4.7 is higher for the Y specimens. The surface finish quality of the specimens affects the elongation rates, YS, and UTS values and these mechanical properties increase with improved surface finish values.

Table 4.2: Surface Roughness Results of Specimens

Specimen Code	First Trial [µm]	Second Trial [µm]	Third Trial [µm]	Mean Value R_a [µm]
Y (Z-direction)	0.58	0.80	0.56	0.65
D (X-direction)	1.04	0.70	0.14	0.63

The support removal process is also different for D and Y samples because the manufacturing direction is different. Therefore, each specimen has its own support structure. These supports are removed with grinding, stoning, and sandblasting processes. However, the support structure effects occur in each specimen. Therefore, the roughness results differ in specific locations.

In Alok Gupta, Chris J. Bennett, and Wei Sun's research [6] it was reported that the surface roughness affects the YS and UTS values and also changes the ductility of the material. Therefore, the elongation rate changes according to the surface finish process. When the full of internal pored specimens are machined, the pores will move to the surface and decreases the fatigue performances, and cause detrimental effects [6].

4.3. Hardness Test of Specimens

A Hardness Test is a useful method to examine the static strength of the materials. In this thesis for the hardness test, the BMS 200-RBOV hardness tester machine was used. The machine is shown in Figure 4.4 and Figure 4.5. In addition, the diamond cone probe was used for the measurements. The test machine can determine the average of 50 Rockwell (HRC) with a diamond indenter and 200 Brinell with a 2.5mm ball bearing indenter. For this

test, Rockwell (HRC) value was measured because of the limitations of Ti-6Al-4V mechanical properties. The Ti6Al4V Grade 5 Powder has 36-41 Rockwell (HRC) and 379 Brinell values. Therefore, the tester cannot provide Brinell value but can measure Rockwell (HRC) value.

Figure 4.4: BMS 200-RBOV Hardness Tester

Figure 4.5: Diamond Cone Indenter

The hardness test was done according to ISO 6508-1 standard. The preliminary force of 10kg (98.07N) was maintained for a duration of 2 seconds. Then, the total test force of 150 kg (1.471kN) was maintained after 1-5 seconds. Then, the measurement was read. The three measurements were done from the gripping area of both vertically and horizontally manufactured specimens. The measurement points can be seen in Figure 4.6. The hardness test results are shown in Table 4.3.

Figure 4.6: Hardness measurement points

Table 4.3: Rockwell Hardness Results of Specimens

Specimen Code	Measurement 1	Measurement 2	Measurement 3	Average
D (X-direction)	28 HRC	28 HRC	28 HRC	28 HRC
Y (Z-direction)	31 HRC	31 HRC	31 HRC	31 HRC

According to the measurements, the vertically built specimens (Y) are a higher Rockwell C hardness value than the horizontally built specimens (D). These results support the YS and UTS values of the vertically and horizontally built specimens that are shown in Table 4.7. The vertically built specimens (Y) have better YS and UTS values than the horizontally built specimens (D). However, both of the specimens have lower Rockwell C values than the pure Ti-6Al-4V Grade 5 (36-41 HRC). Therefore, EBM-built specimens become softer than the pure Ti6Al4V alloys.

The lower HRC value of the Ti6Al4V Grade 5 that is observed can be ascribed to the existence of the porosities and α and β phases or related artifacts during manufacturing.

However, for the pure Ti6Al4V, the Rockwell Hardness value was marginally higher than the additively manufactured specimens [58].

4.4. Microstructure Texture

Before the investigation of the microstructure texture of the parts, the cutting, surface quality, and preparation processes need to be done according to demanded texture quality. The first process of microstructure texture is the sensitive cutting process. This process was done in the sensitive cutting machine Brilliant 220 which is shown in Figure 4.7 and the view of the specimen after cutting process is shown in Figure 4.8.

Figure 4.7: Brilliant 220 Sensitive Cutting Machine

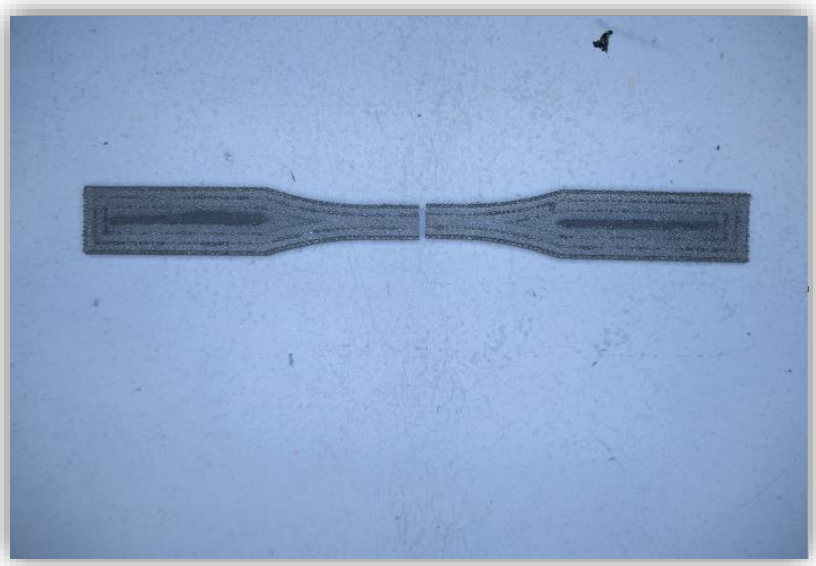

Figure 4.8: Sensitive Cut Point of Specimens

After the cutting process, the pieces are located into the Bakelite in Ecopress 50 machine which is shown in Figure 4.9. This process is required for the grinding and polishing process because the dimensions of the cutting pieces are very small, so Bakelite makes it easier to polish the pieces. The piece in Bakelite is shown in Figure 4.10.

Figure 4.9: Ecopress 50 Bakelite Machine

Figure 4.10: Piece of Specimen in Bakelite

The third process of the microstructure texture is the sanding and polishing process. In this process, the pieces surface quality in Bakelite is increased within the polishing process. This process provides better surface quality and also minimizes the effect of manufacturing remnants. Within this process, the microstructure texture of the parts can be seen well. The Sanding and Polishing machine is shown in Figure 4.11.

Figure 4.11: Struers Tegramin 25: Sanding and Polishing Machine

The Final process of the microstructure study is Chlorine analyzing process. In this process, the pieces are exposed to Chlorine for 10 seconds. This process provides a better

microstructure analysis opportunity because chlorine opens the pores of the microstructure of specimens. After this process, the pieces are studied in a microscope LEICA DM2700M which is shown in Figure 4.12. While scanning the microstructure of the specimens', the yellow-colored filter is used to take clear images in the microscope.

Figure 4.12: LEICA DM2700M - Microscope

The mechanical properties of Ti6Al4V, which is manufactured by the EBM process change among the sources. The process parameters like scanning speed, pre-heating, beam current, and also building direction has a direct effect on the final static and dynamic mechanical properties because of the anisotropic microstructure of the products.

The microstructure of Ti6Al4V Titanium Alloy includes α and β phases that have a crystal structure with hexagonal close-packed and body-centered cubic respectively. For this Titanium Alloy, Aluminum is used to balance α phases at higher temperatures; however, Vanadium is used to balance the β phase at lower temperatures [60]. The microstructure of the specimens can be examined when the planes are parallel oriented to building directions.

The specimens that were manufactured with 185x20x2.5mm are cut from the midpoints vertically and the microstructure of the specimens that were manufactured in two

directions is studied. When the microstructure of the Ti6Al4V is examined, α + β phases are dominant, however, the α phase seems less than the β phases in the middle regions of the specimens. α + β alloys like Ti6Al4V can be controlled by HIP to adjust the β phases of the parts. This provides some advantages in the mechanical properties of the parts and also the α + β materials show good manufacturing properties, high strength in the room, and moderately elevated temperatures [61].

In Figure 4.13 and Figure 4.14, the dark places represent α phases and the light places represent β phases. The grain size of the Ti6Al4V differs in different locations because of the α + β pattern. The vertical grains can affect the specimens' mechanical properties because of the building directions. The Y specimens have lower elongation rates. In addition, the grain direction of the specimens can be associated with the tensile properties of the Ti6Al4V. The α and β phases of D and Y specimens can be seen in Figure 4.13 and Figure 4.14.

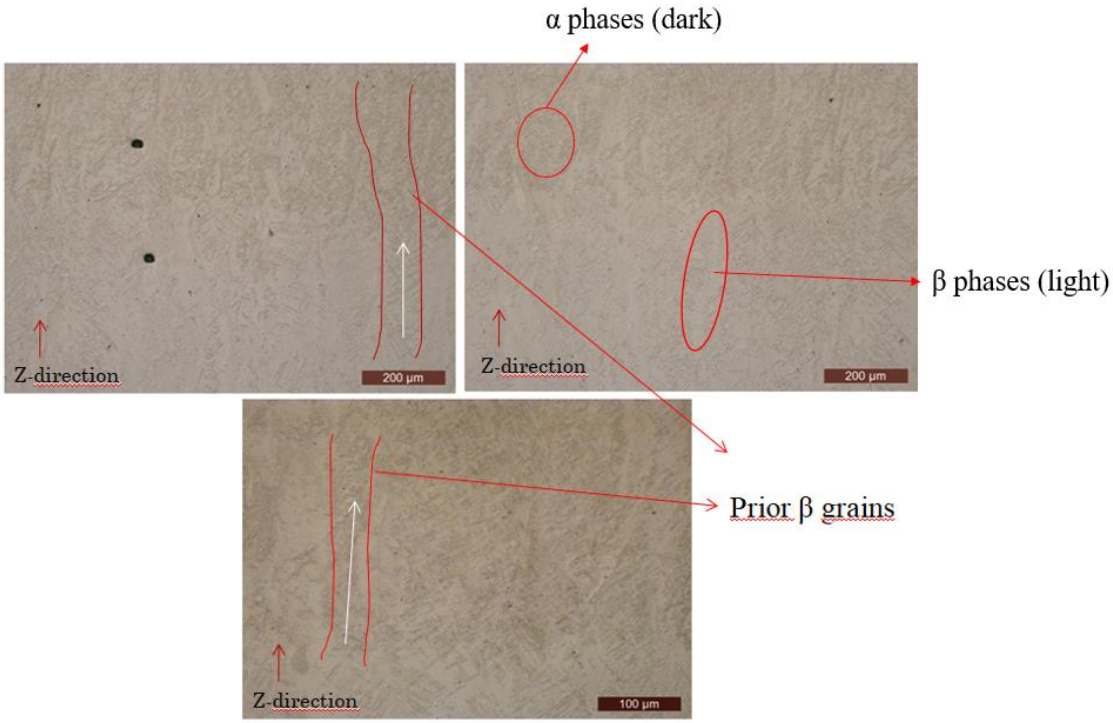

Figure 4.13: Y Specimens α and β Phase Texture

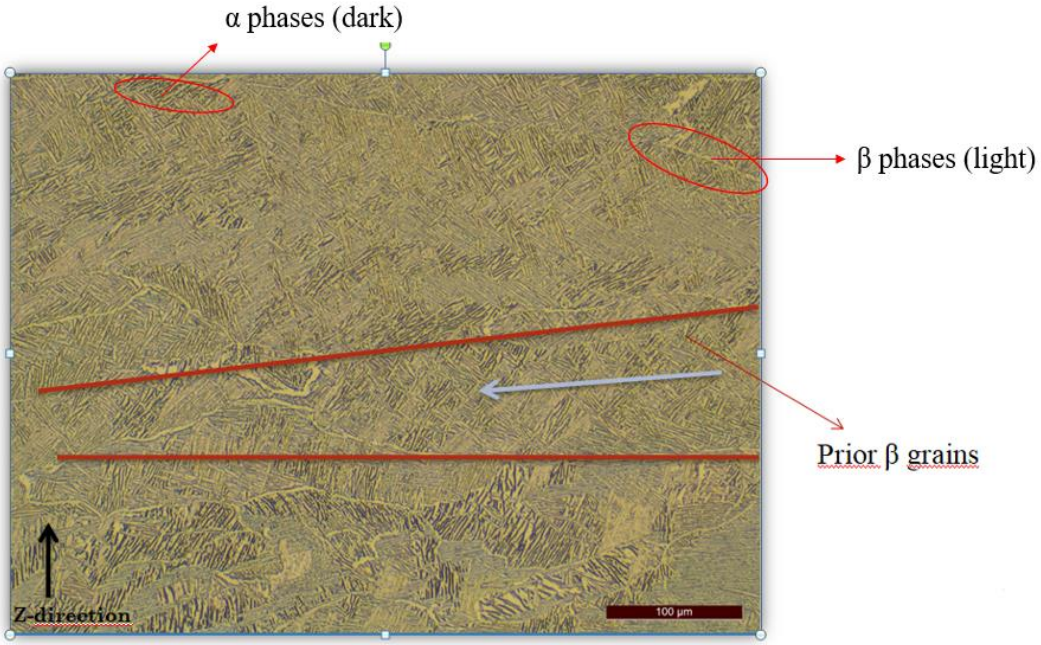

Figure 4.14: D Specimens α and β Phase Texture

Y (Vertically Manufactured) specimens have higher hardness values than D (Horizontally Manufactured) specimens. When the microstructures of these specimens are examined, the α phase seems thinner in the Y specimens' microstructure and α phases support the higher hardness value of vertically manufactured specimens.

The prior β grains symbolize the manufacturing direction of the specimens. For D specimens the grain direction seems as vertical, for Y specimens the direction seems as horizontal to the manufacturing direction. The α + β microstructure transition was seen in the prior β grain microstructure. The Y specimens have lower elongation rates compared to the D specimens because the grain direction of the Y specimens is parallel to the tensile load.

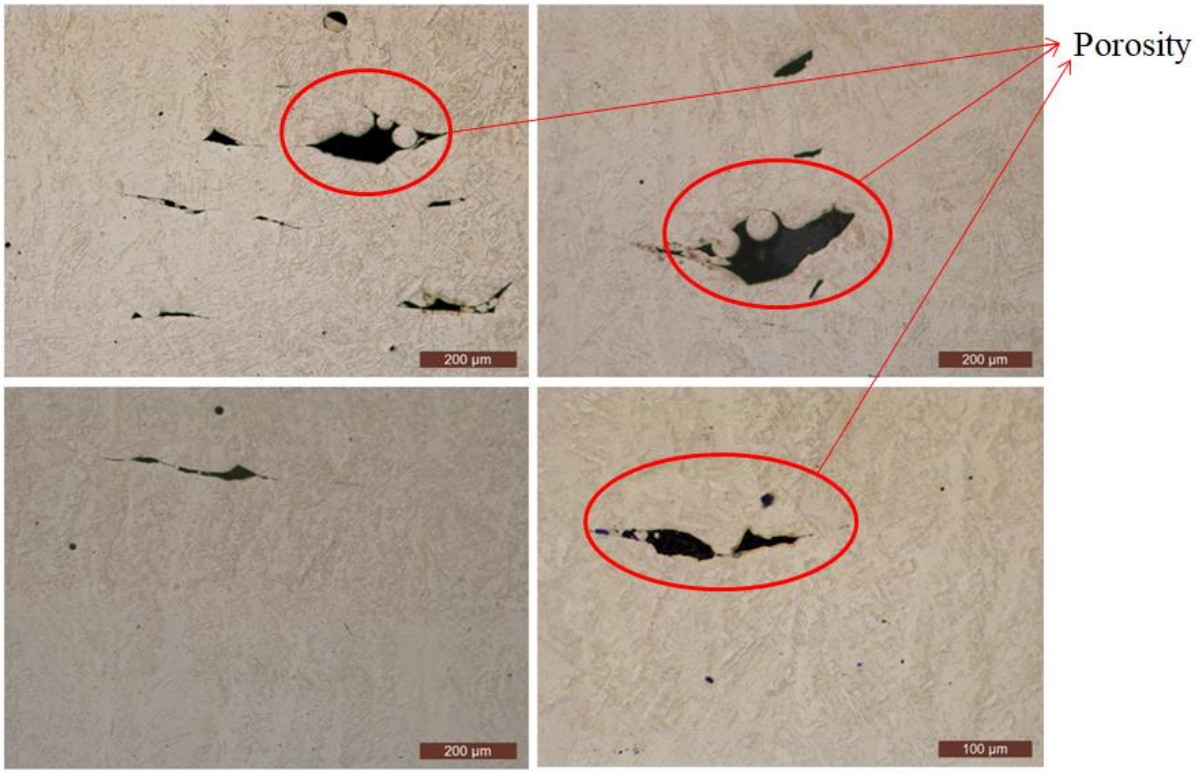

Figure 4.15: Y Specimens Porosity Texture

According to the microstructures of the Y and D specimens, the porosities can be indicated in texture. Therefore, these porosities in the structure decrease the strength properties of the parts. The porosity pattern is not homogeneous and its size and location change according to the manufacturing. It causes a decrease in YS, UTS, and E values because it affects the strength of the material in specific locations. The porosity pattern of the parts can be seen in Figure 4.15 and Figure 4.16.

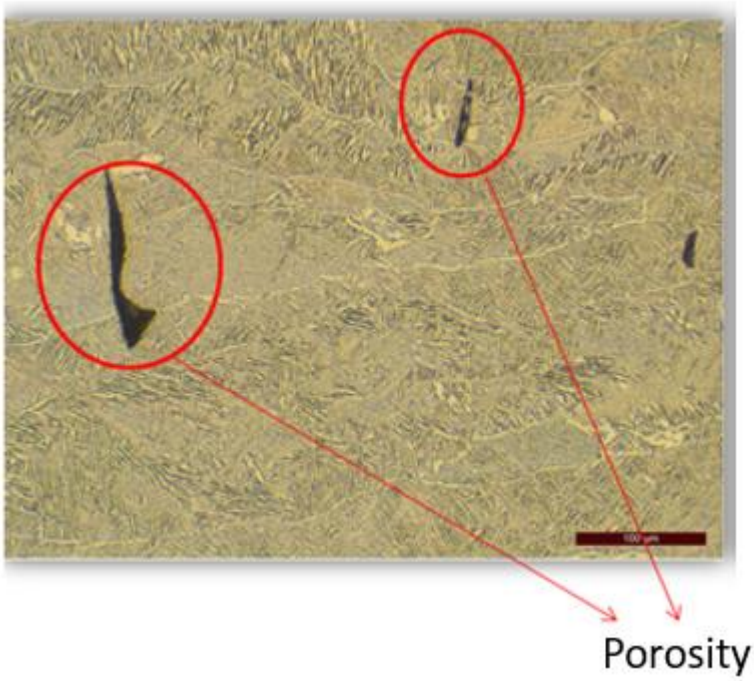

Figure 4.16: D Specimens Porosity Texture

4.5. Quasi-Static Tensile Test Method and Parameters

The quasi-static or uniaxial tensile test is the most important and the most frequently used mechanical test worldwide, which determines the strength and elongation parameters for the applications of metals, which are of decisive importance for the design and construction of components, everyday objects, machines, vehicles, and structures. The test task is to determine material parameters reliably and reproducibly and to ensure international comparability.

The uniaxial tensile test is a method of determining characteristic values for yield point or yield stress, tensile strength, modulus of elasticity, Poisson ratio, and elongation at break. Additionally, lower yield point, yield point elongation, and elongation at maximum force are also determined.

As stated in section 3.2.1, the specimens were manufactured according to ASTM E8 standard. The Ti6Al4V grade 5 powder is used for specimen manufacturing and the dimensions of the powder are around 45-106 μm. ASTM E8 / E8M standard allows the use of different specimen types like bars, sheets, tubes, and round specimens for testing options

(See Figure 4.17). However, the rectangular specimens are mostly used in the tensile tests with a width of 12.5 mm and gauge length of 50 mm [62].

Figure 4.17: ASTM E8 Test Specimen Standard [62]

The tensile test was performed according to the test standard ISO 6892-1 for the tension testing. The tests have been performed at room temperature and 50% humidity. Zwick Roell Z250 with a gauge length of 50mm has been used to measure the specimens' Elongation Point ($R_{p0.2}$), Tensile strength (R_m), Young Modulus (E), Elongation at fracture (A). The machine parameters are shown in Table 4.4. The tensile test setup is shown in Figure 4.18 and Figure 4.19. The fractured test specimens are shown in Figure 4.20.

Table 4.4: Zwick/Roell Z250 Machine Parameters

Model	**Zwick Z250**
Maximum Test Force (tensile / compression) [kN]	250
Maximum crosshead travel [mm]	320
Test speed [mm/min]	0,0005...600
Force measurement accuracy with load cell	from 0,5 kN class 1 from 2,5 kN class 0,5

Figure 4.18: Zwick/Roell Z250 Tensile Test Machine

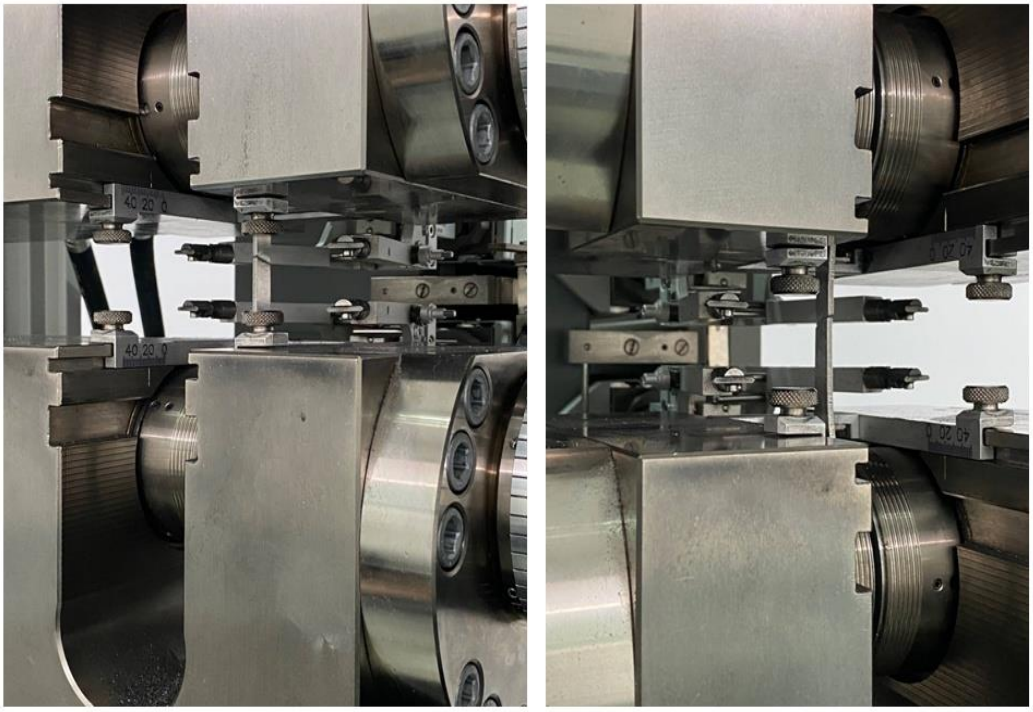

Figure 4.19: Tensile Test of Specimens

Figure 4.20: Fractured Specimens After Six Tensile Tests

4.5.1. Tensile Test Results

Here, the vertically (Z-direction) manufactured test specimens are coded as Y1, Y2, and Y3 while the horizontally (X-direction) manufactured test specimens are coded as D1, D2, and D3.

The test results were collected via an electronic system that is connected to the test machine. The numerical and graphical results of the six specimens can be seen in this section. Yield strength (Rp0.2), Tensile strength (Rm), Young Modulus (E), Elongation (elastic and plastic) (At (corr.)), Gauge Length (L0), Specimen Thickness (a0), and center width (b0) are shown in Table 4.5 and Table 4.6. The Y and D specimens' stress and elongation graphs are shown in Figure 4.21 and Figure 4.22.

Table 4.5: Vertically (Z-direction) manufactured test specimens (Y1, Y2 and Y3).

Legends	Specimen Code	E (GPa)	$R_{p0.2}$ (MPa)	R_m (MPa)	A_t (corr.) %	L_0 mm	a_0 mm	b_0 mm
Red	Y1	111.017	793.5	895.1	10.4	25	2.51	10.78
Green	Y2	104.979	820.1	938.2	9.0	25	2.28	10.46
Blue	Y3	102.311	830.8	925.5	12.1	25	2.52	10.66

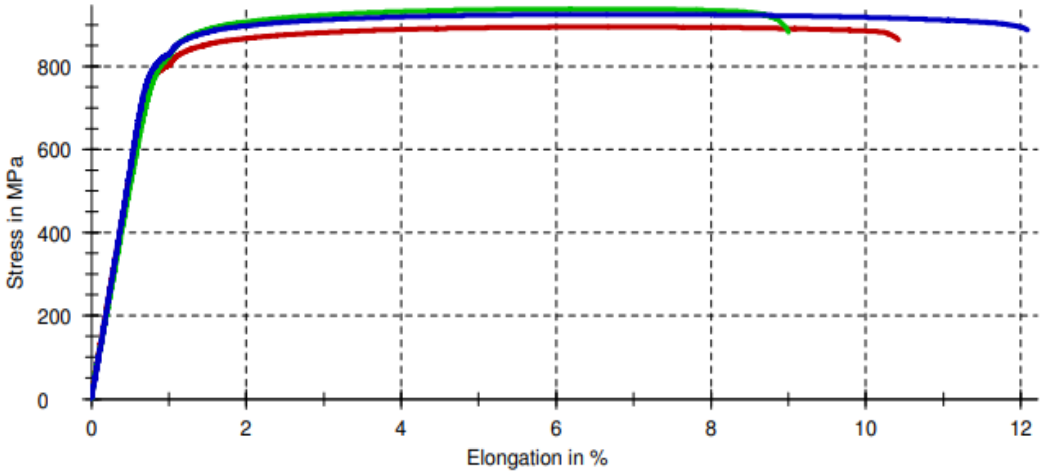

Figure 4.21: Y1, Y2 and Y3 specimen Stress and Elongation graph

Table 4.6: Horizontally (X-direction) manufactured test specimens (D1, D2 and D3).

Legends	Specimen Code	E (GPa)	$R_{p0.2}$ (MPa)	R_m (MPa)	A_t (corr.) %	L_0 mm	a_0 mm	b_0 mm
Red	D1	103.967	810.4	909.5	12.6	25	2.53	9.85
Green	D2	104.650	778.7	893.4	13.8	25	2.56	9.94
Blue	D3	108.611	823.5	928.6	14.8	25	2.33	9.93

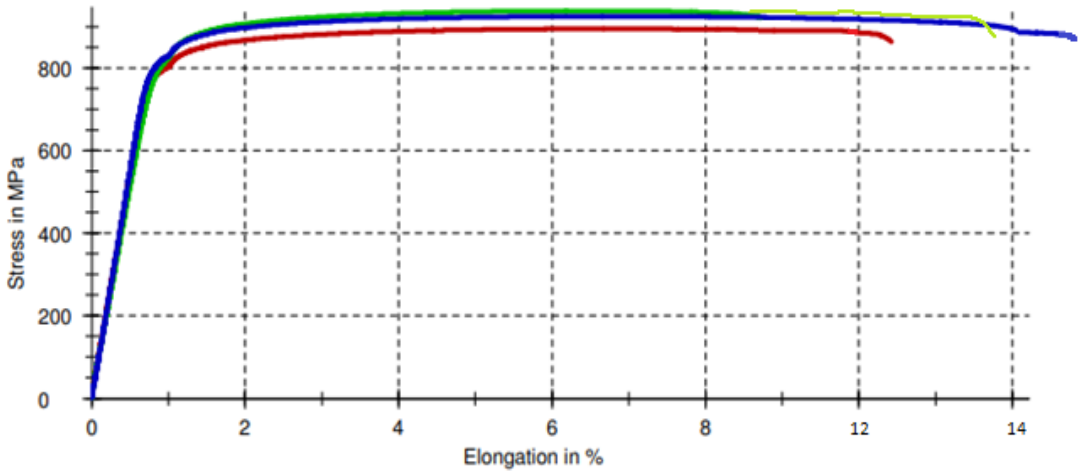

Figure 4.22: D1, D2 and D3 specimen Stress and Elongation graph

The uniaxial tensile test results of Ti-6Al-4V Grade 5 specimens in the form of rectangular cross section that were produced in the vertical and horizontal building directions are shown in Table 4.7. The Powder, Cast and Wrought Ti6Al4V mechanical properties are also given to make comparison among Titanium Alloys.

Table 4.7: Tensile test Results and Comparison with Titanium Alloys.

Specimen Code	Young's Modulus [GPa]	YS (Offset 0.2%) [MPa]	UTS [MPa]	Elongation %
Ti6Al4V Grade 5 Powder (GE Comp.)	120	951	1020	14
Cast Ti6Al4V Material (ASTM F1108)	114	758	860	> 8
Wrought Ti6Al4V Material (ASTM F1472)	114	860	930	> 10
Y Specimens (Z-direction)	106.1	814.8	919.6	10.5
D Specimens (X-direction)	105.75	804.2	910.5	13.7

The tensile test results show that the strength values of the rectangular samples that are produced in vertical and horizontal directions are close to each other. However, the vertically manufactured samples (Y Specimens) are more brittle than horizontally

manufactured (D Specimens) samples. The Y Specimens have lower elongation rates than the D specimens. (See Table 4.7)

In addition, the horizontal and vertical specimens are compared with the Ti6Al4V Grade 5 Powder, Cast, and Wrought Titanium in Table 4.7. The table shows that the Y and D specimens have better YS, UTS, and elongation rates than that of Cast Ti6Al4V. However, their YS, UTS, and elongation rates are less than the corresponding values of Ti6Al4V Powder and Wrought Ti6Al4V. In fact, the difference between the values of wrought titanium and the specimens tested is in the range of 1-2%. The difference between strength and elongation values is affected because of the machining parameters like the scanning speed, beam current, heat values, and also manufacturing technique. As stated in the microstructure inspection part, the specimens that are manufactured by the EBM method have porosities in their microstructures. Therefore, the static and dynamic mechanical properties show a difference compared with values for the block materials. In addition, the powder dimensions also affect the microstructure because the process parameters are selected according to the powder dimensions and the material so, the microstructure and the density of the specimens are affected. The tensile strength of the Y and D specimens decreases because of the presence of the porosities that are discussed in the previous section. In conclusion, the process parameters, manufacturing technique, powder properties, and microstructure affect the mechanical properties of the specimens used in this thesis.

According to the work reported in ref [6], the rectangular dog-bone specimens show similar mechanical properties with the horizontally manufactured rectangular blocks and the vertically build cylindrical specimens. In their research, the overall Yield Strengths of the vertical cylindrical specimens and the horizontal rectangular specimens were 761 MPa and 744 MPa, respectively. The corresponding values in this study are 814.8 MPa and 804.2 MPa, respectively. The Ultimate Tensile Strength of the vertically manufactured cylindrical specimens and the horizontally manufactured rectangular specimens were 842 MPa and 838 MPa in ref [6]. In the present study corresponding UTS values were 919.6 MPa and 910.5 MPa respectively. According to these results, the rectangular dog-bone Y and D specimens have higher strength values than the results reported by Gupta et al [6].

In addition, in their research [6], they observed that the build direction also affects the yield and ultimate tensile properties. The vertically manufactured specimens have higher

YS and UTS compared to the horizontally manufactured specimens. These results are consistent with the results reported in ref [6]. However, the horizontally manufactured specimens are more brittle than the vertically manufactured specimens. The vertically manufactured specimens lack fusion areas that are perpendicular to the load axis and the stress concentration locations that cause premature failure because of reduced ductility [6].

In the microstructure texture of the Y and D specimens, the porosities can be seen in texture. Therefore, these porosities cause lack of fusion areas in the structure so, the static and dynamic mechanical properties of the specimens are affected because of the improper fusion areas. When the microstructures of these specimens are examined, the α phase seems thinner in the Y specimens' microstructure and α phases support the higher hardness value of vertically manufactured specimens. The manufacturing direction of the Y specimens have perpendicular to the load axis in the quasi-static tensile tests; therefore, it is expected that the elongation value is lower than the corresponding value of X specimens. Due to the higher hardness value of Y specimens, it becomes more brittle than X specimens. Therefore, the microstructure of the specimens also supports the results.

It can be concluded here that the Y and D specimens' tensile test results show similarities with the results reported in ref [6]. The Y (vertically built) specimens have better YS and UTS than D (horizontally built) specimens. The mechanical property differences between Gupta et al. [6] specimens' and D & Y specimens tested in this thesis are around 9-10%. The differences occur because of the powder layer thickness, manufacturing parameters, etc. They used 70-200 μm powder size and Arcam A2XX EBM machine for the production of the specimens. However, in this thesis, 45-106 μm powder size and Arcam Q20 Plus EBM machine were used.

According to the results, the research shows that the machine parameters, design shapes, and powder dimensions affect the mechanical properties. In the thesis, the dog-bone rectangular Y and D specimens manufactured indicate better mechanical properties than the results reported in ref [6].

5. HIGH STRAIN RATE TESTS

5.1. Split-Hopkinson Pressure Bar Test Description

The Hopkinson Pressure Bar (HBB) test is a widely used technique to determine the high-velocity deformation properties and structural equations of materials. Compression, tensile, shear, and bending tests can be performed at high speeds with this test method which is developed on the basis of the principle of unidirectional elastic wave transmission in long bars. When combined with numerical methods, the HBB test method provides researchers with a simple and economical method for determining the impact phenomena in the laboratory and verifying the material structural equations in a short time [63].

The Hopkinson test set up contains a gas gun, a striker rod, Teflon bearings, shock absorbers, a multiplier, incident and transmitting bars, and a data collection unit that are shown in Figure 5.1. A portion of the unidirectional stress wave (depending on the mechanical impedance of the material under test) is generated by the impact of the striking rod against the field rod, which is thrown from the gas gun at different velocities [63].

Calculations are made with the assumption of unidirectional movement of elastic stress waves in long rods. The amount of stress in the area bar varies with the ejection speed of the striking bar and the modulus of elasticity and elastic wave speed of the bar material. The time interval of the elastic wave on the field rod depends on the striking rod length and the elastic wave speed. The elongation of the field rod and conducting rod is calculated by the amount of incoming, returning, and transmitted strains. The stress formed in the sample changes with the amount of transmitted strain and the cross-sectional areas of the sample and the bar. The deformation rate of the sample is adjusted by changing the speed of the striking rod [63].

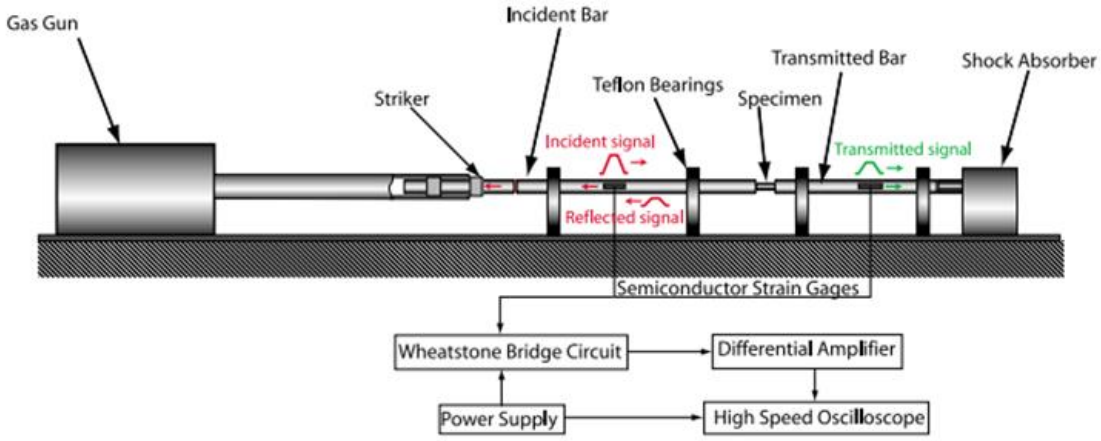

Figure 5.1: Schematic of Split-Hopkinson Pressure Bar used in experiments [64]

With the HBB setup, the compressive stress-strain behavior of the materials at different deformation rates like low and high speeds and the wave transition in multi-layer materials can be determined. When combined with static velocity experiments, structural equations can be created. In addition to the compression test, high-speed tensile, shear, and bending tests can also be performed on the HBB assembly with appropriate modifications. High and low-temperature mechanical tests and adiabatic heating measurements of the sample during deformation were also developed in the HBB setup [65]. Damages at high deformation rates can be determined by using a fast camera [66].

The tested samples of strain rate (έ), the strain (ε), and the stress (σ) can be calculated by using the following equations: [67]

$$\acute{\varepsilon}(t) = -\frac{2C_b}{L_s}\varepsilon_r(t) \tag{5.1}$$

$$\varepsilon(t) = -\frac{2C_b}{L_s}\int_0^t \varepsilon_r(t)\,dt \tag{5.2}$$

$$\sigma(t) = \frac{A_b E_b}{A_s}\varepsilon_t(t) \tag{5.3}$$

where C_b is the elastic wave velocity of the bar, L_s is the sample length, A_s and A_b are the sample and bar cross- sectional areas, ε_i, ε_r, and ε_t are, respectively, the incident, reflected and transmitted strains that are measured from strain gages mounted on the bar. [67]

The equations that are shown above are drawn based on the test assumptions according to the sample and HBB bars force interfaces. The force equation of the specimens can be expressed by equation 5.4 [68].

$$R = \frac{2(F_1 - F_2)}{F_1 + F_2} \quad (5.4)$$

where F_1 and F_2 are the front and back surface forces on the Split-Hopkins Bar setup. The number R is a measure of the deviation from stress equilibrium in the specimen. When the value of R that is expressed in equation 5.4 reaches 0, the stress equilibrium in the setup is reached [68].

T. Zhou et al. [69] stated that the EBM Ti6A14V specimens were imposed to compressive deformation at under high strain rates. In his investigation, the compression tests were performed to obtain dynamic mechanical properties of specimens for strain rate range of 1.0×10^{-3} s^{-1} to 1.0×10^{3} s^{-1}.

The strain rate for this test has five different intervals for quasi-static and high strain ranges

- Low strain rate ranges from 1.0×10^{-4} s^{-1} to 1.0×10^{-2} s^{-1},
- Medium strain rate ranges from 1.0×10^{-2} s^{-1} to 1.0×10^{-1} s^{-1},
- High strain rate ranges from 1.0×10^{-1} s^{-1} to 1.0×10^{2} s^{-1},
- Ultra-high strain rate is 1.0×10^{2} s^{-1} to 1.0×10^{4} s^{-1} and beyond 1.0×10^{4} s^{-1} [70].

5.2. Specimen Manufacturing and Preparation

The specimens are manufactured from Electron Beam Melting Technology with the same Powder (GE Company Ti6Al4V Grade 5) that is used for tensile test specimens. However, the specimens that were used for Split-Hopkins Bar Test were manufactured vertically and horizontally with the diameter of 8mm. The specimens' examples are shown in Figure 5.2.

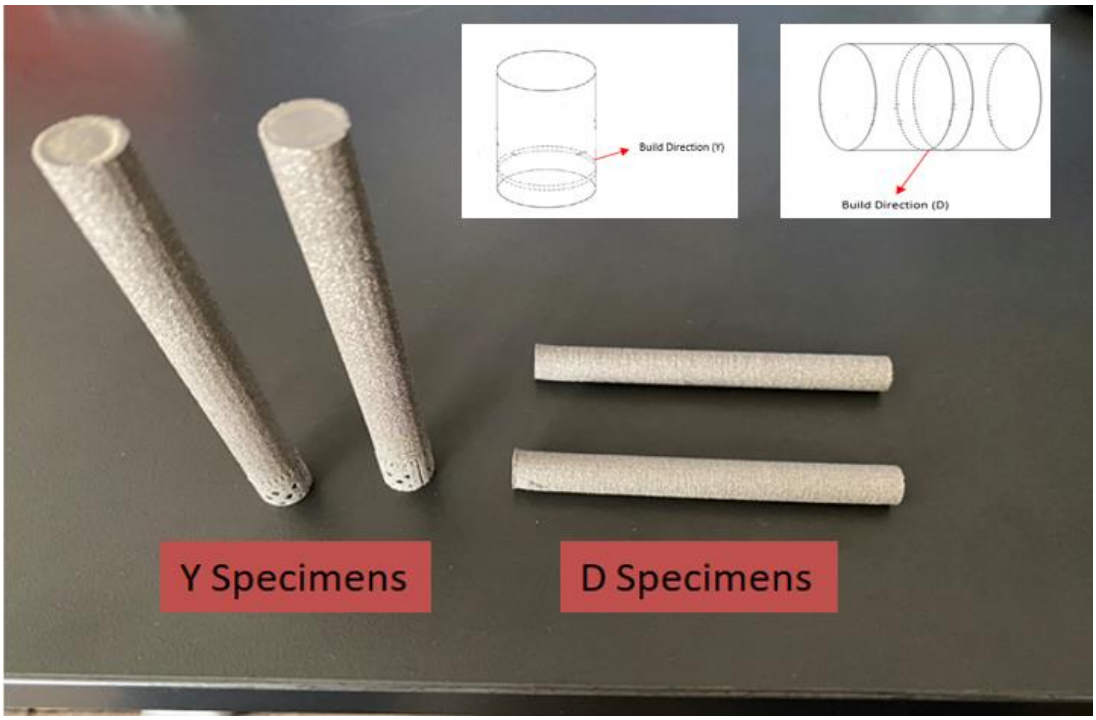

Figure 5.2: Schematic of Split-Hopkinson Pressure Bar Specimens After Manufacturing

The vertically manufactured specimens have a support structure on the beginning side of the manufacturing, however, the horizontally manufacture specimens have a support structure on the lateral faces. The EBM machine starts production from the outer to the inside of the specimens, Therefore, the surface of the specimens has powder remnants and bad surface quality. In order to remove the remnants of the powder and reach a good surface quality, the grinding and turning processes were carried out on the specimens' surface in a lathe. In addition, the specimens were cut equally into 24 pieces for the Split-Hopkins Bar Tests. The appearance of the specimens after surface processes can be seen in Figure 5.3.

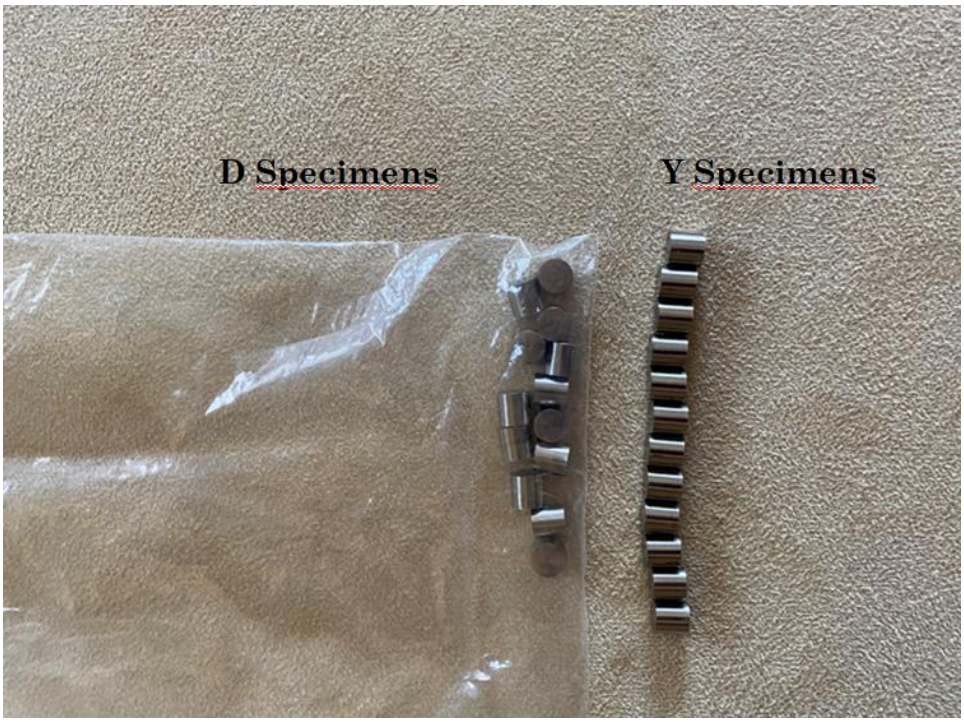

Figure 5.3: D and Y Specimens for Split-Hopkinson Bar Test

The test specimens are compressed with the REL Split-Hopkinson Pressure Bar setup which is shown in Figure 5.4. The test platform consists of an automated compression accelerator with 36-inch barrels, C350 Compression Bar Set with Strikers and a Momentum Trap, a Data acquisition package, a stop and stands with hydraulic energy absorption, and a 200 Psi air compressor [71]. The specimens are located between the bars which is shown in Figure 5.5.

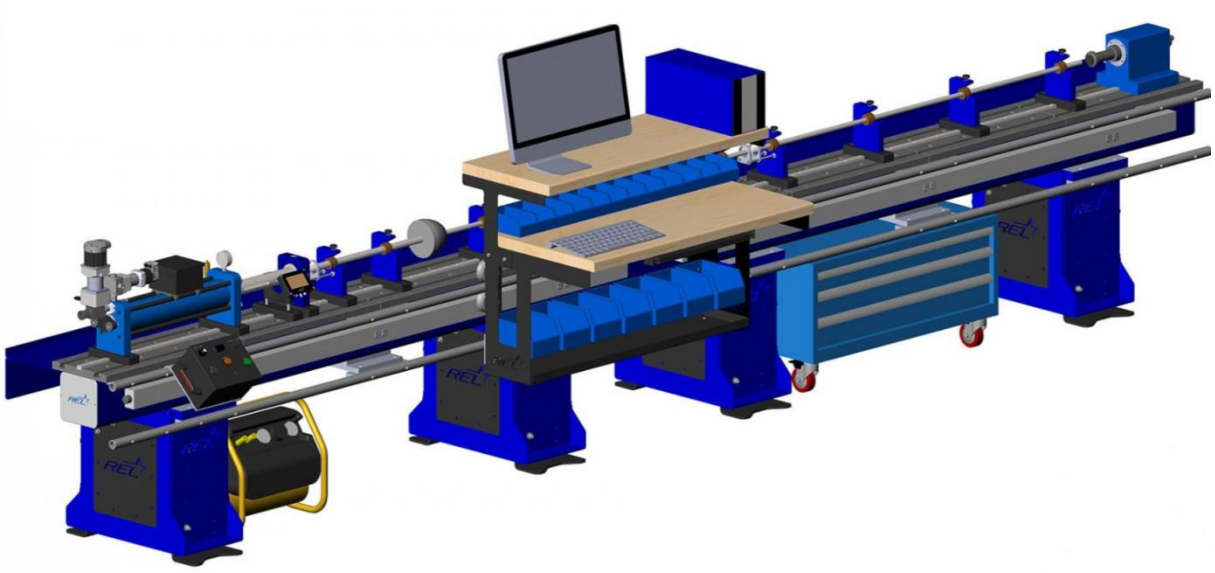

Figure 5.4: SHPB Compression System REL [71]

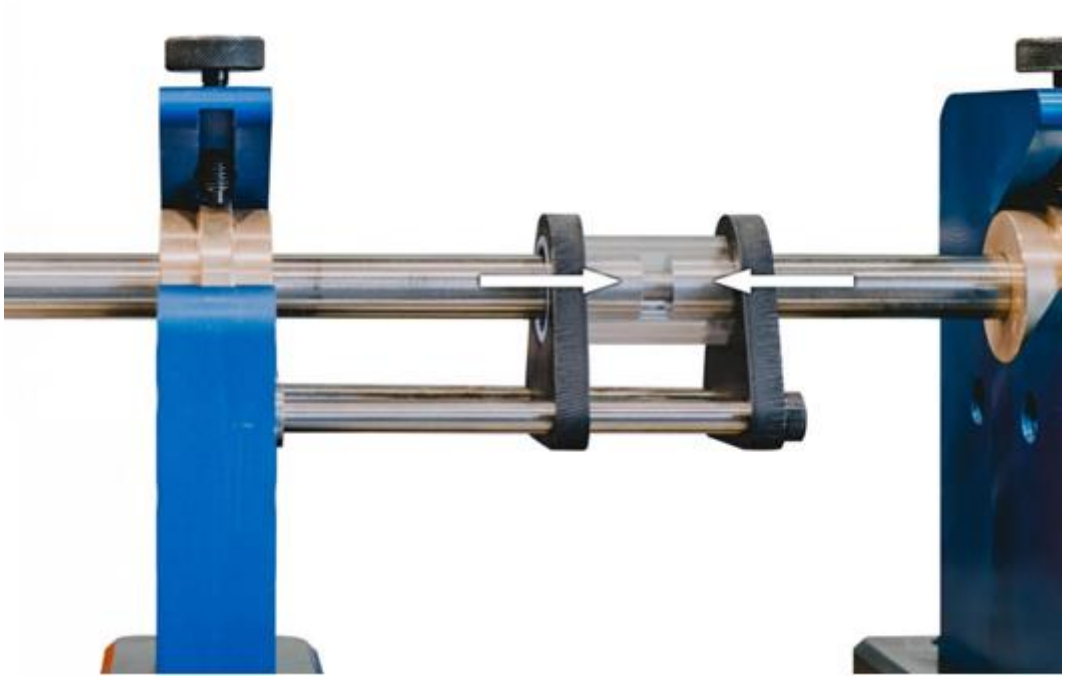

Figure 5.5: SHPB Compression System Specimen Location [71]

5.3. SHPB Compression Test Results

During the test, vertically and horizontally manufactured specimens are used for different pressure values. The speed is controlled by the pressure difference. For this test, the high and ultra-high strain rate intervals are used for h ranges. The pressures are selected as 15, 45, and 75 psi respectively. The initial diameters and lengths are measured for all the specimens before the test. After the test, the final diameters, lengths, and speeds are taken from the test. The test data for the Y and D Specimens can be seen in Table 5.1 and Table 5.2. According to the test data, the strain rate vs. time, stress vs. time, strain vs. time, and stress vs. strain graphs were obtained. The SHPB test results are shown in Figure 5.6 to Figure 5.17.

Table 5.1: Y Specimens Hopkinson Test Parameters (Vertically Manufactured)

Specimen Code	Initial Diameter (mm)	Initial Length (mm)	Final Diameter (mm)	Final Length (mm)	Striker Bar Length (mm)	Pressure (Psi)	Temperature (C°)	Speed (m/s)
Y1	6.05	6.10	6.04	5.98	300	15	25	7.852
Y2	5.85	6.05	6.05	5.97	300	15	25	8.065
Y3	6.00	6.11	6.11	5.63	300	45	25	13.76
Y4	6.03	6.11	6.11	5.50	300	45	25	13.59
Y5	6.03	6.10	6.10	5.23	300	75	25	17.51
Y6	5.97	6.07	6.07	5.43	300	75	25	17.47

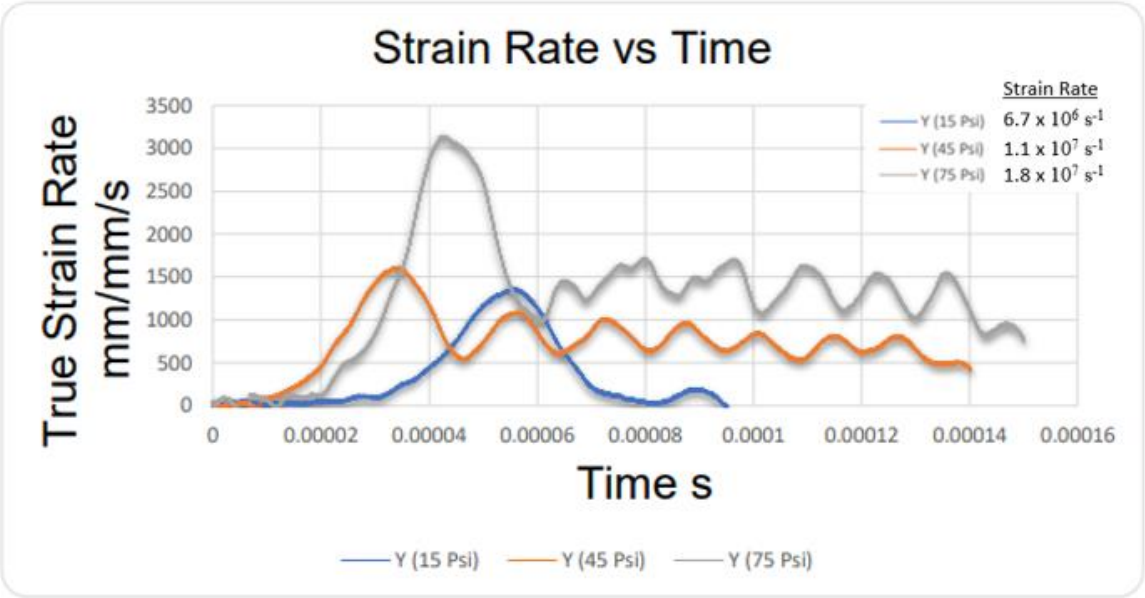

Figure 5.6: Y specimens 15,45,75 Psi Strain Rate vs. Time Graph

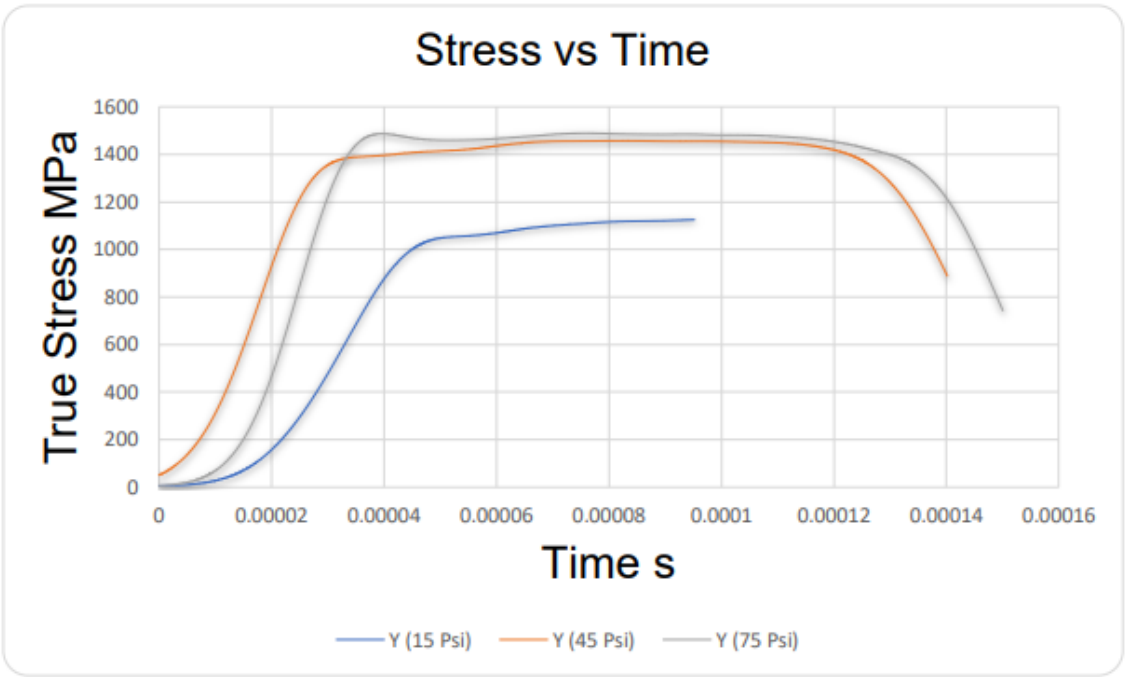

Figure 5.7: Y specimens 15,45,75 Psi Stress vs. Time Graph

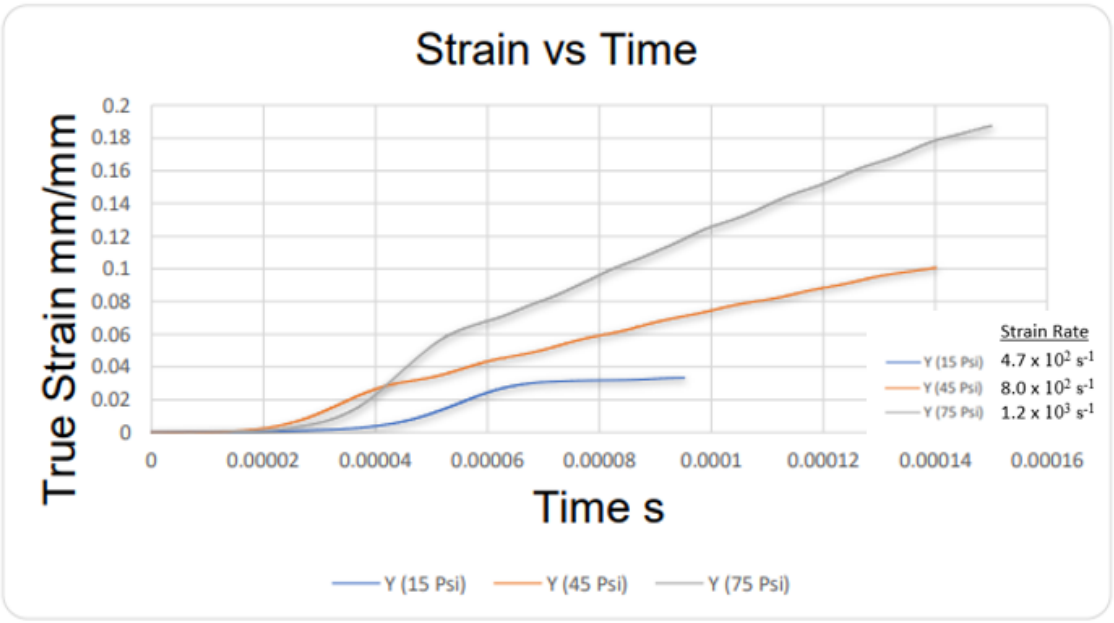

Figure 5.8: Y specimens 15,45,75 Psi Strain vs. Time Graph

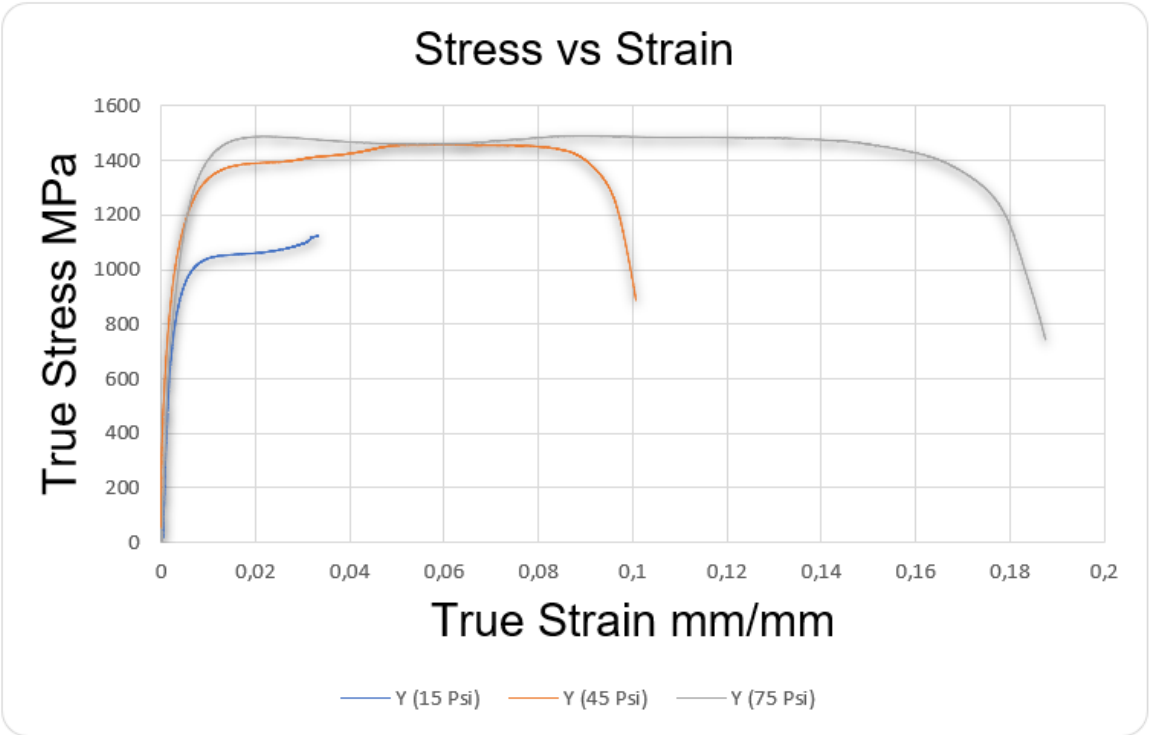

Figure 5.9: Y specimens 15,45,75 Psi Stress vs. Strain Graph

Table 5.2: D Specimens Hopkinson Test Parameters (Horizontally Manufactured)

Specimen Code	Initial Diameter (mm)	Initial Length (mm)	Final Diameter (mm)	Final Length (mm)	Striker Bar Length (mm)	Pressure (Psi)	Temperature (C°)	Speed (m/s)
D1	5.98	6.28	6.02	6.00	300	15	25	8.108
D2	5.89	5.99	5.93	5.88	300	15	25	7.942
D3	5.95	5.96	6.24	5.57	300	45	25	13.68
D4	5.96	6.05	6.21	5.67	300	45	25	13.50
D5	5.88	6.02	6.40	5.24	300	75	25	17.43
D6	5.94	6.18	6.41	5.38	300	75	25	17.08

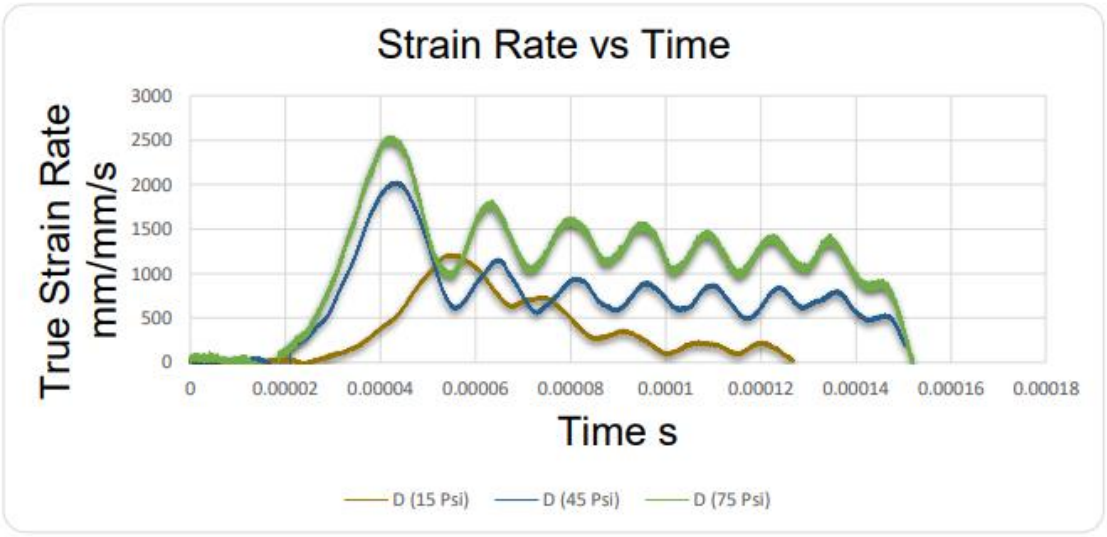

Figure 5.10: D specimens 15,45,75 Psi Strain Rate vs. Time Graph

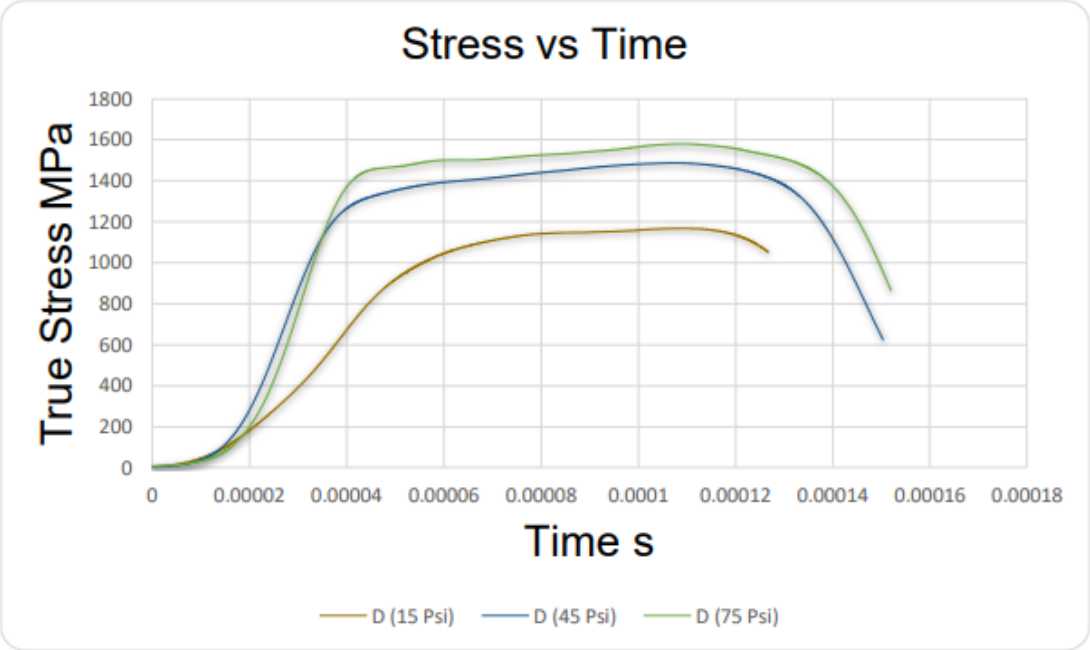

Figure 5.11: D specimens 15,45,75 Psi Stress vs. Time Graph

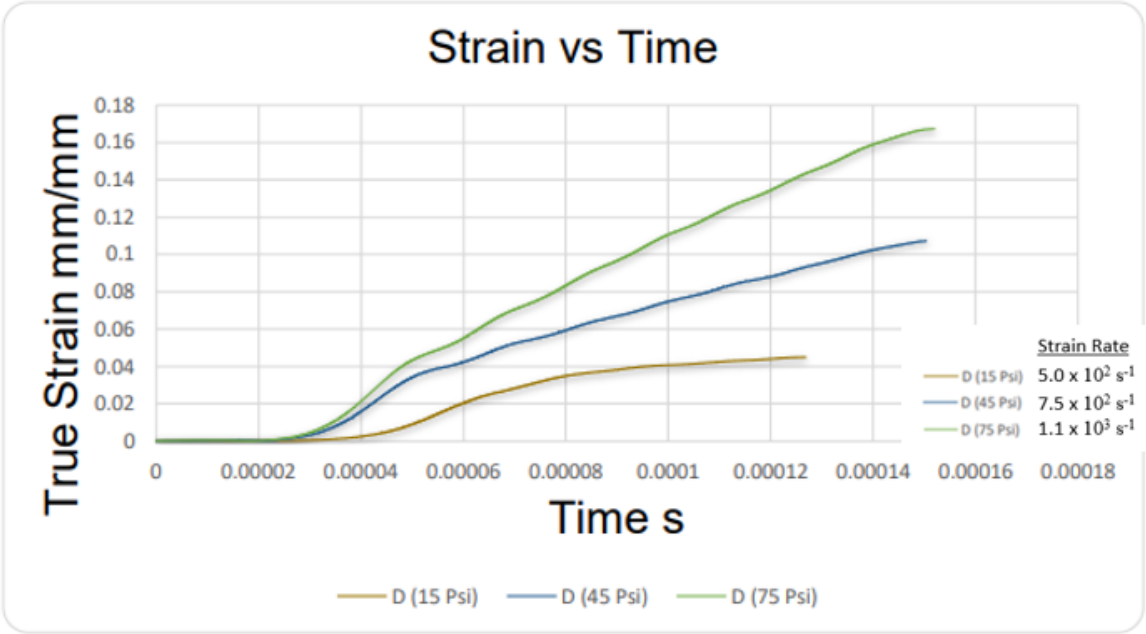

Figure 5.12: D specimens 15,45,75 Psi Strain vs. Time Graph

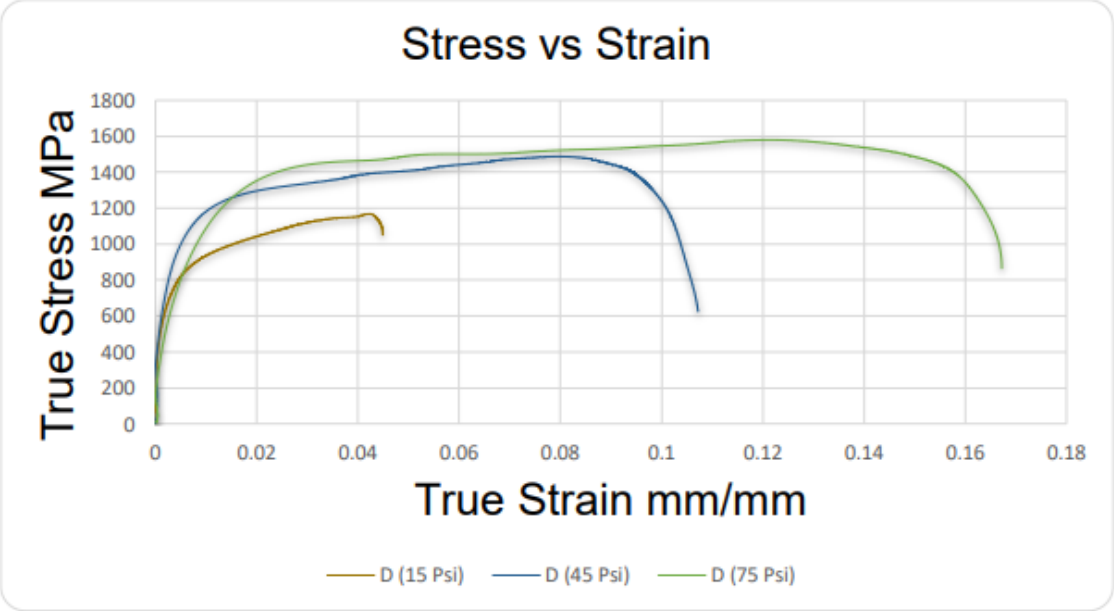

Figure 5.13: D specimens 15,45,75 Psi Stress vs. Strain Graph

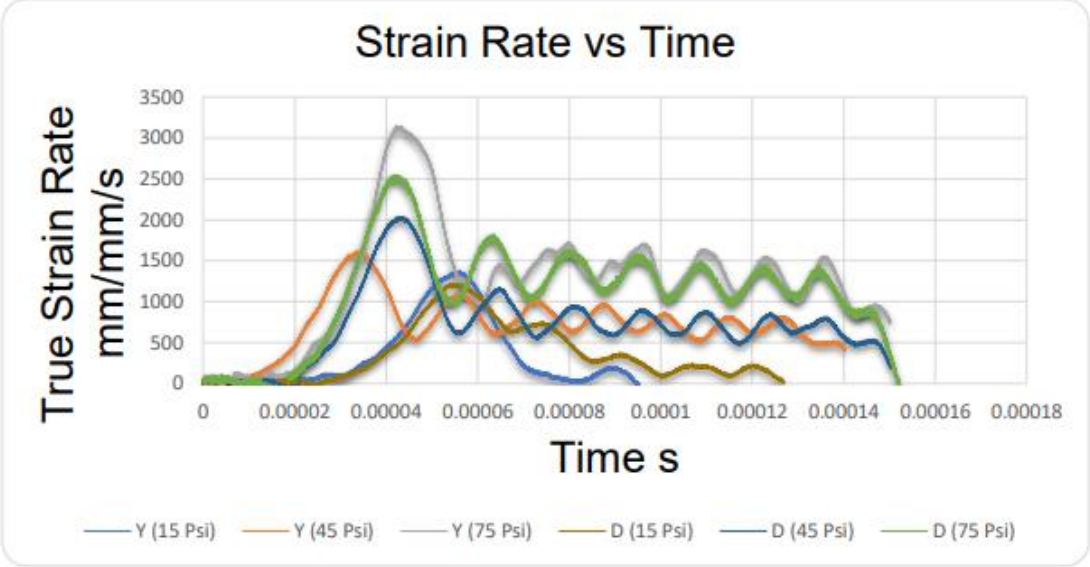

Figure 5.14: Y specimens 15,45,75 Psi and D specimens 15,45,75 Psi Strain Rate vs. Time Graph

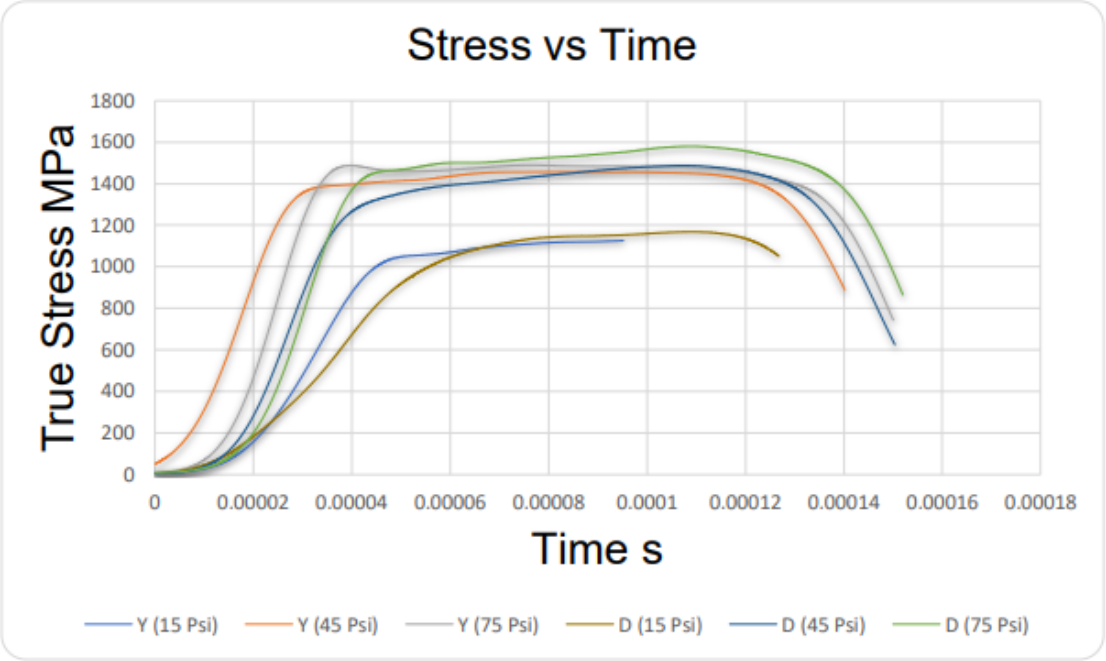

Figure 5.15: Y specimens 15,45,75 Psi and D specimens 15,45,75 Psi Stress vs. Time Graph

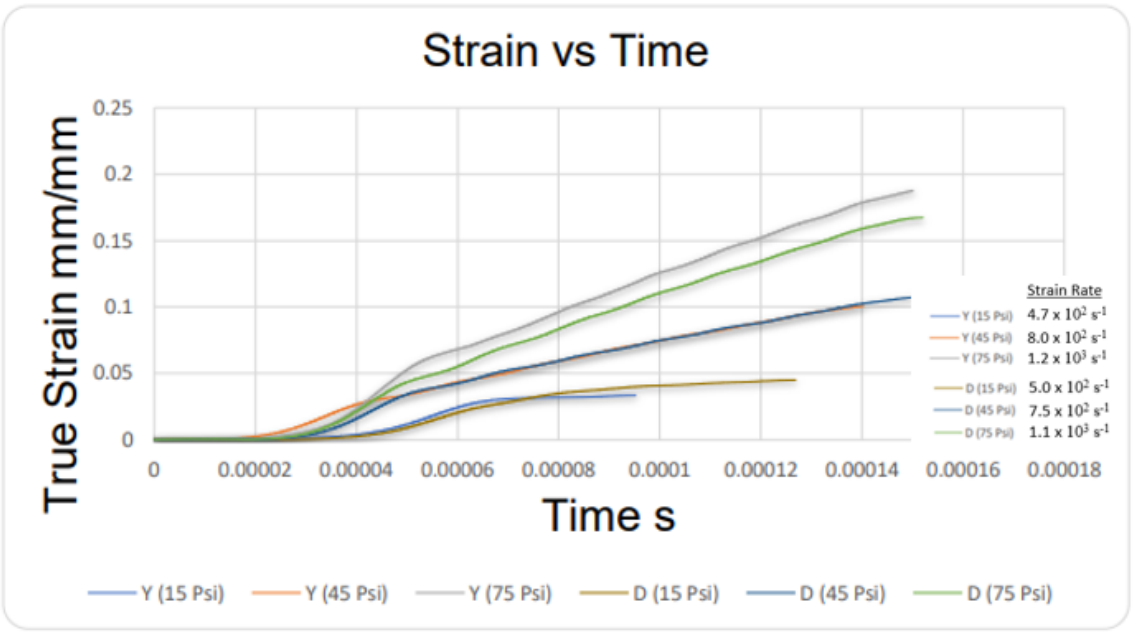

Figure 5.16: Y specimens 15,45,75 Psi and D specimens 15,45,75 Psi Strain vs. Time Graph

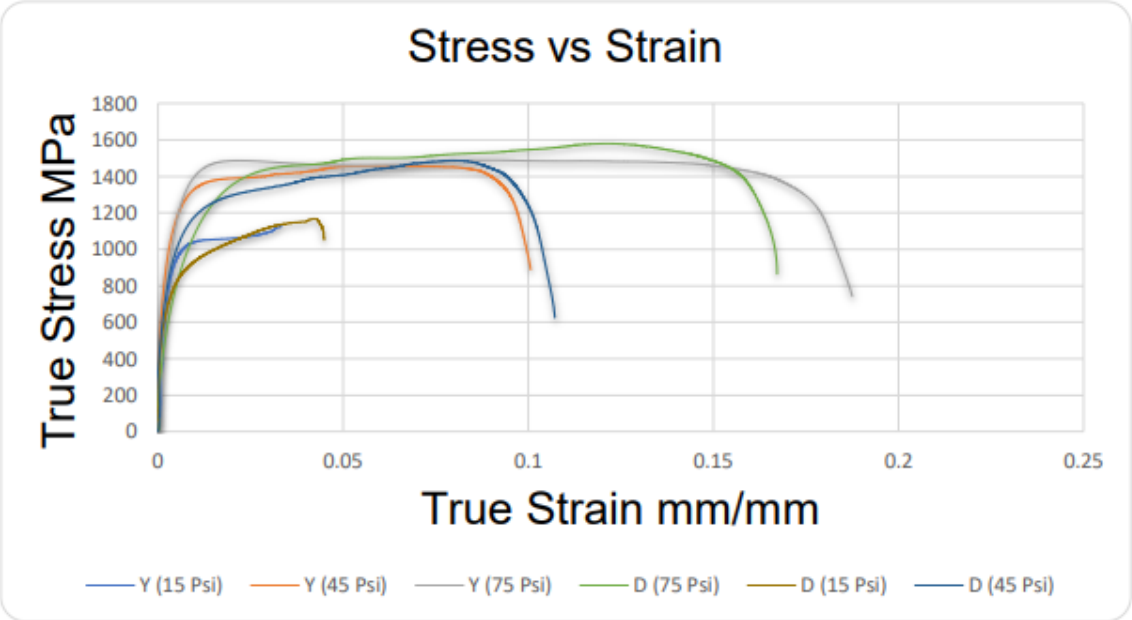

Figure 5.17: Y specimens 15,45,75 Psi and D specimens 15,45,75 Psi Stress vs. Strain Graph

For the SHPB test results, the test results were obtained from data collection units of the SHPB machine. The graphs that are shown above are comprised of pulse signals that are collected by the strain gauges of the test setup. In addition, the Striker Bar length that is shown in Table 5.1 and Table 5.2 affects the strain rate results of the specimens. However, it was selected as 300mm for the whole test.

To obtain the test data graphs, the incident, reflected, and transmitted waves are adjusted to achieve truer data. The specimens are tested in high and ultrahigh strain rates and the speed of the test is adjusted with pressure variance. It is seen that the pressure difference affects the stress, strain, and strain rate of the specimens. Besides, the final diameters become higher and the final lengths become lower with the increase in pressure. According to the results, the UTS of the specimens increases when the strain rate increases. In addition, the plastic deformation stage of the specimens starts when the strain rate becomes 1.0×10^3 s^{-1}.

For the Y specimens, the strain rates can be seen as 4.7×10^2 s^{-1}, 8.0×10^2 s^{-1} and 1.2×10^3 s^{-1} for the pressures of 15, 45 and 75 Psi respectively. In addition, the ultimate stress values become 1130 MPa, 1430 MPa and 1520 MPa according to the related strain rates. It is shown that, when the pressure is increased, the strain rates and true stress values also increase.

For the D specimens, the strain rates can be seen as 5.0 x 10^2 s^{-1}, 7.5 x 10^2 s^{-1} and 1.1 x 10^3 s^{-1} for the pressure of 15, 45 and 75 Psi respectively. In addition, the ultimate stress values become 1180 MPa, 1490 MPa and 1580 MPa according to the related strain rates.

For the comparison of the results for Y and D specimens, the same strain rates are selected to compare the ultimate tensile stress values of the specimens. The results are shown in Table 5.3.

Table 5.3: Y and D Specimens SHPB Ultimate Stress Comparison in Same Pressure and Strain Rate

Specimen Code	**Pressure (Psi)**	**Strain Rate (s^{-1})**	**Ultimate Stress (MPa)**
Y	15	4.7 x 10^2	980
	45	8.0 x 10^2	1400
	75	1.2 x 10^3	1510
D	15	5.0 x 10^2	860
	45	7.5 x 10^2	1320
	75	1.1 x 10^3	1380

According to the test results, it is seen that there is a difference between the Ultimate Stress values for Y (vertically manufactured) and D (horizontally manufactured) specimens. The vertically manufactured Y specimens have higher ultimate stress (around 7-8%) values and are in the same strain rate and pressure conditions. In addition, when the test pressure is increased, the adiabatic heat of the specimens is increased because of the heat accumulation of the shear band. In addition, the Ultimate Stress decreases because of heat accumulation and thermal softening. When the pressure is increased during the tests, the strength values show that the material strength and the pressure values are directly proportional to each other. Therefore, the stress values of the specimens increase according to the pressure value.

In S. Gangireddy et al. research [7], the Ti6Al4V dynamic compression behavior, the horizontal and vertical specimens were manufactured with 5mm diameter. Dynamic compression tests were performed in their research on specimens at a strain rate of 1500 s^{-1} using an SHPB system. According to the results, both as-built horizontal and vertical

specimens show high strength values between 1600 and 1700 MPa [7]. The vertical and horizontal specimens' True Stress vs. True Strain results are shown in Figure 5.18. The V, D, C, X and O letters symbolize manufacturing locations of specimens that were specified in Figure 1.3.

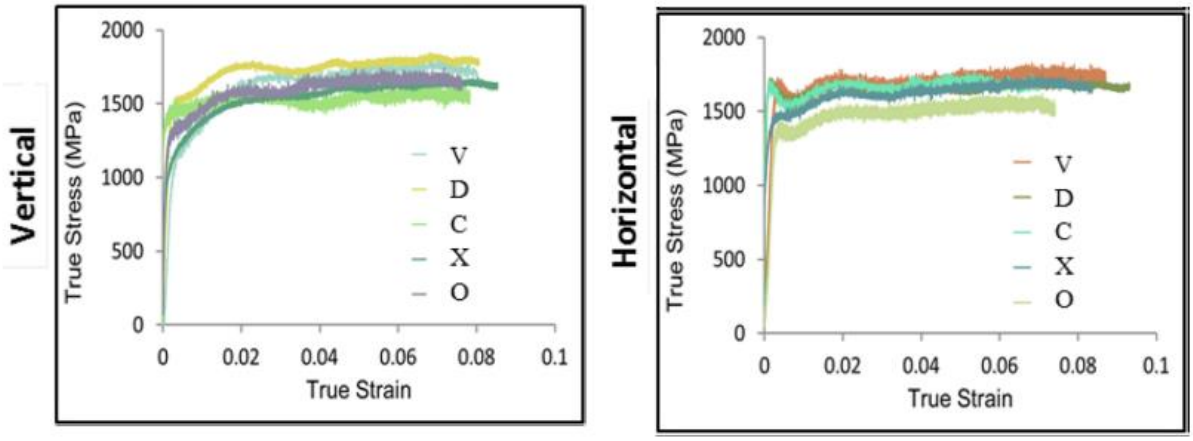

Figure 5.18: Dynamic true stress–true strain curves of the five locations of S. Gangireddy et al. research [7].

The vertically manufactured specimens have better stress values than the horizontally manufactured specimens. The When research results reported in [7] are compared to the results of this thesis, it is clearly seen that the built direction has an effect on material properties at high-strain values. Therefore, the built direction effect starts from low-strain rates and continues to high-strain rates.

In T. Zhou et al. research [69], the dynamic compression shear of the Ti6Al4V at high and ultra-high strains were studied. The specimens were manufactured vertically. The SHPB tests were conducted between 5.0 x 10^2 and 9.0 x 10^3 high and ultra-high strain rates. The results are given in Table 5.4 and Figure 5.19.

Table 5.4: Ultimate stress of specimen under high strain rate of T. Zhou et al. research [69]

Strain rate ($\times 10^2\ s^{-1}$)	5.0	10.0	50.0	70.0	90.0
Ultimate stress (MPa)	1359	1449	1467	1527	1576

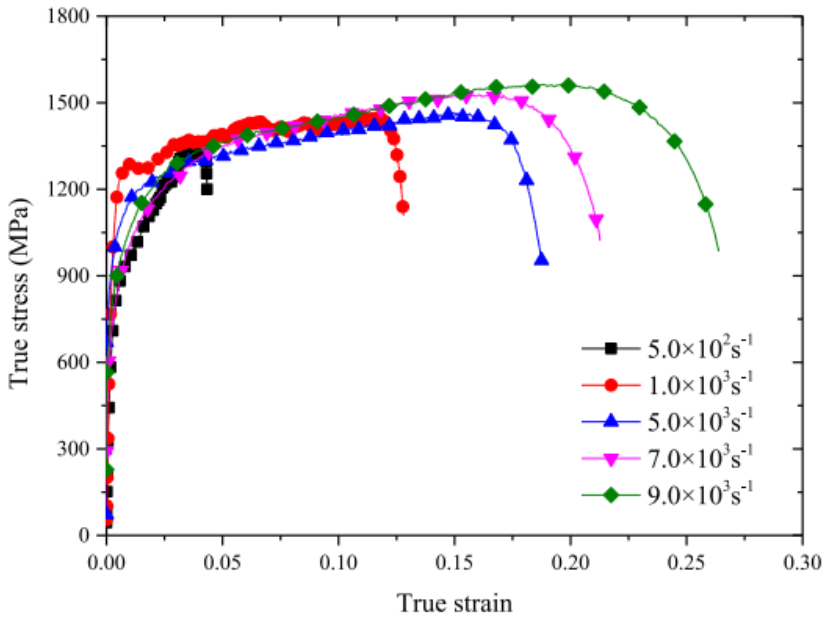

Figure 5.19: True stress-strain curves of SHPB compression test under high strain rate of T. Zhou et al. research [69]

According to the T. Zhou et al. research [69] results, the Ultimate Stress increases directly within strain rate increase. When the Table 5.3 and Table 5.4 are compared, Y and D specimens have 1510 and 1380 MPa Ultimate Stress value at 1.2 x 10^3 and 1.1 x 10^3 strain rate respectively. In T. Zhou et al. results, the vertical specimens have 1449 MPa Ultimate Stress at 1.0 x 10^3 strain rate. Therefore, T. Zhou et al. results support the results in section 5. As a result, the vertically built specimens show higher Ultimate Stress value at similar strain rates compared to horizontally built specimens.

6. CONCLUSION AND FUTURE WORK

In this study, the mechanical properties of the parts that are manufactured from Ti6Al4V Grade 5 Powder in different building directions by the Electron Beam Melting technique were studied. Since the purpose of the thesis is to evaluate the effects of building direction on the static and dynamic mechanical properties of the Ti6Al4V alloy, the test specimens are manufactured in two different directions which are horizontal and vertical because of the research about building direction effect on mechanical properties of Ti6Al4V. By using these specimens, the density measurements, surface roughness measurements, tensile tests, hardness tests, microstructure texturing observations, and the high and ultra-high strain rate compression tests were carried out.

- According to the test results obtained in this thesis, the following conclusions can be drawn;
- The vertically manufactured parts (Y Specimens) have higher YS, UTS, and Elastic Modulus than horizontally manufactured parts (D specimens). However, the vertically manufactured specimens have lower elongation rates than the horizontally manufactured specimens.
- The Y and D specimens have better yield, ultimate tensile strength, and elongation rates than Cast Ti6Al4V; however, they have a lower YS, UTS and elongation rates than that of Ti6Al4V Powder Grade 5 and Wrought Ti6Al4V. However, the difference between the values for the wrought titanium and the specimens tested is in the range of 1-2 %.
- According to the measurements, the vertically built specimens (Y) have higher Rockwell C hardness values than the corresponding values of the horizontally built specimens (D). The vertically built specimens (Y) have higher YS and UTS values than the horizontally built specimens (D). However, both of the specimens have a lower Rockwell C value than that of the pure Ti-6Al-4V Grade 5 33 HRC. Therefore, the EBM-built specimens are softer than the values of Ti-6Al-4V alloy.
- The vertically (Y specimens) manufactured specimens have lower mean surface roughness values compared with the horizontally (D specimens) manufactured specimens. The D specimens have lower surface roughness; therefore, the elongation rate is higher than the corresponding value of the Y specimens.

- The Ti6Al4V specimens have α + β dominant microstructure. The Y (Vertically Manufactured) specimens have higher hardness values compared to D (Horizontally Manufactured) specimens. When the microstructures of these specimens are examined, the α phase seems thinner in the Y specimens' microstructure and α phases support the higher hardness value of vertically manufactured specimens.
- The Ti6Al4V parts can be manufactured by EBM technology by optimizing the process parameters to obtain better mechanical properties.
- The Y specimens show higher UTS values compared to the D specimens under ultra-high strain rates.
- The BCC (body-centered cubic) crystal structure of the Ti6Al4V offers higher mechanical properties. This structure consists of the β phase. It provides more planes to deform the titanium alloy. Therefore, the volume fraction of the α and β phases have an effect on the tensile properties of Ti6Al4V.
- The strength properties of the Ti6Al4V increase while the pressure increases in compression tests.
- According to the thesis results, the designs can be formed pursuant to vertical manufacturing constraints under both compressive and tensile loads because vertically built specimens' mechanical properties are close to the required powder mechanical properties.

The following topics can be studied as future work over this study:

- The fatigue and dynamic properties of Ti6Al4V are manufactured in different building directions by Electron Beam Melting technology.
- The effect of the HIP process on microstructure and mechanical properties of Ti6Al4V manufactured by AM technology.
- FEM analysis can be carried out by using the data obtained from SHPB tests.
- Using the SHPB test set up a tensile high strain rate test can be carried out and the material model can be developed.

REFERENCES

[1] N. Kara, “Havacılıkta Katmanlı İmalat Teknolojisinin Kullanımı,” Mühendis ve Makina, vol. 636, no. 54, pp .70-75, 2013.

[2] H. Bikas, A. K. Lianos, and P. Stavropoulos. "A design framework for additive manufacturing." The International Journal of Advanced Manufacturing Technology, vol. 103 no. 9, pp. 3769-3783, 2019.

[3] C. Klahn, B. Leutenecker, and M. Meboldt. "Design strategies for the process of additive manufacturing." Procedia Cirp, vol. 36, pp. 230-235, 2015.

[4] S. Rawal, J. Brantley, and N. Karabudak. "Additive manufacturing of Ti-6Al-4V alloy components for spacecraft applications." 2013 6th international conference on recent advances in space technologies (RAST), IEEE, pp. 5-11, 2013.

[5] V. Chastand, et al. "Fatigue characterization of Titanium Ti-6Al-4V samples produced by Additive Manufacturing." Procedia Structural Integrity 2, vol. 1, pp. 3168-3176, 2016.

[6] A. Gupta, C. J. Bennett, and W. Sun. "The role of defects and characterisation of tensile behaviour of EBM Additive manufactured Ti-6Al-4V: An experimental study at elevated temperature." Engineering Failure Analysis, vol. 120, pp. 5-24 February 2021, doi: 105115.

[7] S. Gangireddy, E. J. Faierson, and R. S. Mishra. "Influences of post-processing, location, orientation, and induced porosity on the dynamic compression behavior of Ti–6Al–4V alloy built through additive manufacturing." Journal of Dynamic Behavior of Materials vol. 4 no. 4, pp. 441-451, 2018.

[8] S. L. Draper, B. A. Lerch, J. Telesman, R. E. Martin, A. J. Ring, I. E. Locci, and A. Garg, "Materials Characterization of Electron Beam Melted Ti-6Al-4V," The NASA Scientific and Technical Information (STI), Hampton, 2016.

[9] E. H. Nava, A study on the mechanical properties of micro-truss Ti-6Al-4V materials fabricated by Electron Beam Melting, Ph.D. thesis: The University of Sheffield, United Kingdom, 2016.

[10] G. Mandil, van Thao Le, H. Paris, and M. Sua, "Building new entities from existing titanium part by electron beam melting: microstructures and mechanical properties," Le Centre pour la Communication Scientifique Directe, 2015.

[11] H. Galarragaa, D. A. Ladosa, R. R. Dehoffb, M. M. Kirkab, and Peeyush Nandwana, "Effects of the microstructure and porosity on properties of Ti-6Al-4V ELI alloy fabricated by electron beam melting (EBM)," Additive Manufacturing, vol. 10, pp. 47- 57, 2016.

[12] P. Edwards, A. O'Conner, and M. Ramulu, "Electron Beam Additive Manufacturing of Titanium Components: Properties and Performance," Journal of Manufacturing Science and Engineering, vol. 135, 2013.

[13] C. Formanoir, S. Michotte, O. Rigo, L. Germain, and S. Godet, "Electron beam melted Ti–6Al–4V: Microstructure,texture and mechanical behavior of the as-built and heattreated material," Materials Science&Engineering, vol. 652, pp. 105-119, 2015.

[14] Z. Yuwei, H. Galarraga, D. A. Lados., "Microstructure Evolution, Tensile Properties, and Fatigue Damage Mechanisms in Ti-6Al-4V Alloys Fabricated by Two Additive Manufacturing Techniques," Procedia Engineering, vol. 114, pp. 658-666, 2015.

[15] H. Nikolas, & T. Quinn. “Effects of processing on microstructure and mechanical properties of a titanium alloy (Ti–6Al–4V) fabricated using electron beam melting (EBM), part 1: Distance from build plate and part size.” Materials Science and Engineering: A, vol. 573, pp. 264-270, 2013, doi:10.1016.

[16] E. P. A. O’Conner, & M. Ramulu. “Electron Beam Additive Manufacturing of Titanium Components: Properties and Performance.” Journal of Manufacturing Science and Engineering, vol. 135 no.6, 2013, doi:10.1115/1.4025773.

[17] R. Wauthle., B. Vrancken, B. Beynaerts, et al. “Effects of build orientation and heat treatment on the microstructure and mechanical properties of selective laser melted Ti6Al4V lattice structures. “Additive Manufacturing, 5, 77-84. 2015, doi:10.1016.

[18] H. Gong, T. Starr, K. Rafi, H. Gu, G.D.J Ram, and B. Stucker, "Influence of defects on mechanical properties of Ti–6Al–4 V components produced by selective laser melting and electron beam melting," Materials and Design, vol. 86, pp. 545-554, 2015.

[19] S. T. Yiğitbaşı. “Mechanical properties of Ti6Al4V parts produced by electron beam melting and topology optimization in different building directions.” MSc thesis. Dept. Mechanical Eng., Middle East Technical University, Turkey, 2018.

[20] B. Dutta, et al. "Direct metal deposition." Advanced Materials & Processes vol. 169, no. 8 pp. 33, 2011.

[21] M. F. Zäh, and S. Lutzmann. "Modelling and simulation of electron beam melting." Production Engineering vol. 4, no. 1 pp. 15-23, 2010.

[22] B. Duman, and M. C. Kayacan. "Doğrudan metal lazer sinterleme/ergitme yöntemi ile imal edilecek parçanın mekanik özelliklerinin tahmini." Teknik Bilimler Dergisi vol. 7, no. 1, pp. 12-28, 2017.

[23] A. R. R. Bineli, et al. "Direct metal laser sintering (DMLS): Technology for design and construction of microreactors." 6º CONGRESS OBRASILEIRO DE ENGENHARIA DE FABRICA ÇÃO. vol. 11. April 11-15, 2011.

[24] A. V. Filippov, et al. "On the problem of formation of articles with specified properties by the method of electron beam freeform fabrication." Journal of Physics: Conference Series. Vol. 1115. No. 4. IOP Publishing, 2018.

[25] W. J. Seufzer, and K. M. Taminger. "Control methods for the electron beam free form fabrication process." 2007 International Solid Freeform Fabrication Symposium. United States. 2007.

[26] K. Taminger, and R. A. Hafley. "Electron beam freeform fabrication: a rapid metal deposition process." 3rd annual automotive composites conference. September 9-10, United States. 2003.

[27] M. Izadi, et al. "A review of laser engineered net shaping (LENS) build and process parameters of metallic parts." Rapid Prototyping Journal, vol. 26, no. 6, pp. 1059-1078, 2020.

[28] J. P. Kruth, et al. "Lasers and materials in selective laser sintering." Assembly Automation, vol. 23, no. 4, pp.357-371, 2003.

[29] S. Kumar, "Selective laser sintering: a qualitative and objective approach." Journal of The Minerals, Metals & Materials Society, vol. 55 no. 10, pp. 43-47, 2003.

[30] S. Bremen, W. Meiners, and A. Diatlov. "Selective laser melting: a manufacturing technology for the future?" Laser Technik Journal, vol. 9, no. 2 pp. 33-38, 2012.

[31] M. Brandt, et al. "High-value SLM aerospace components: from design to manufacture." Advanced Materials Research, vol. 633. pp. 135-147, 2013.

[32] T. G. Spears, and S. A. Gold. "In-process sensing in selective laser melting (SLM) additive manufacturing." Integrating Materials and Manufacturing Innovation vol. 5, no. 1, pp. 16-40, 2016.

[33] V. S. Sufiiarov, et al. "The effect of layer thickness at selective laser melting." Procedia engineering vol. 174, pp. 126-134, 2017.

[34] T. DebRoy, et al. "Additive manufacturing of metallic components–process, structure and properties." Progress in Materials Science vol. 92 no. 3, pp. 112-224, 2018.

[35] M. K Imran, S.H. Masood, M. Brandt, S. Bhattacharya, J. Mazumder. “Direct metal deposition (DMD) of H13 tool steel on copper alloy substrate: evaluation of

mechanical properties.” Materials Science and Engineering: A, vol. 528, no. 9, pp. 3342-3349, 2011.

[36] K. Shah, A. J. Pinkerton, A. Salman, L. Li. “Effects of melt pool variables and process parameters in laser direct metal deposition of aerospace alloys.” Material Manufacturing Process, vol. 25. no. 12, pp. 1372–1380, 2010.

[37] B. Baufeld, E. Brandl, O. V. der Biest. “Wire based additive layer manufacturing: comparison of microstructure and mechanical properties of Ti-6Al-4V components fabricated by laser-beam deposition and shaped metal deposition.” Journal of Material Processing Technology, vol. 211, no. 6, pp. 1146–1158, 2011.

[38] T. Wang, Y. Y Zhu, S. Q. Zhang, H. B. Tang, H. M. Wang. “Grain morphology evolution behavior of titanium alloy components during laser melting deposition additive manufacturing.” Journal of Alloys and Compounds, vol. 632, pp. 505–513, 2015.

[39] D. H. Ding, Z. X. Pan, D. Cuiuri, H.J. Li. “Wire-feed additive manufacturing of metal components: technologies, developments and future interests.” The International Journal of Advanced Manufacturing Technology, vol. 81, no. 1, pp. 465–481, 2015.

[40] J. Xiong, Y.Y Lei, H. Chen, G. J. Zhang. “Fabrication of inclined thin-walled parts in multi-layer single-pass GMAW-based additive manufacturing with flat position deposition.” Journal of Materials Processing Technology, vol. 240, pp. 397–403, 2017.

[41] V. Bhavar, P. Kattire, V. Patil, S. Khot, K. Gujar, R. Singh. “A review on powder bed fusion technology of metal additive manufacturing.” 4th International conference and exhibition on additive manufacturing technologies; India, September 1-2, 2014.

[42] T. M. Mower, M. J. Long. “Mechanical behavior of additive manufactured, powder-bed laser-fused materials.” Materials Science and Engineering: A, vol. 651, pp. 198–213, 2016.

[43] D. Herzog, et al. "Additive manufacturing of metals." Acta Materialia, vol. 117 pp. 371-392, 2016.

[44] S. Singh, S. Ramakrishna, and R. Singh. "Material issues in additive manufacturing: A review." Journal of Manufacturing Processes, vol. 25, pp. 185-200, 2017.

[45] B. Leutenecker-Twelsiek, C. Klahn, and M. Meboldt. "Considering part orientation in design for additive manufacturing." Procedia CIRP, vol. 50 pp. 408-413, 2016.

[46] G. Pahl, K. Wallace, Engineering design: A systematic approach, Gerhard Pahl, 3rd Edition, Springer, London, 2007, pp 159-161.

[47] Richtlinie, VDI. “Methodik zum Entwickeln und Konstruieren Technischer Systeme und Produkte.” VDI 2221, pp. 37-89. 2007.

[48] A. Gebhardt, “Understanding Additive Manufacturing: Rapid Prototyping - Rapid Tooling - Rapid Manufacturing,” 1st Edition, Hanser, Munich, 2012. pp. 103-108

[49] Engl. VDI-Gesellschaft Produktion und Logistik, “Additive manufacturing processes, rapid manufacturing - Basics, definitions, processes.” Beuth, Berlin, 2012. pp. 34.

[50] Engl. VDI-Gesellschaft Produktion und Logistik, Part 3, “Additive manufacturing processes, rapid manufacturing - Design rules for part production using laser sintering and laser beam melting,” Beuth, Berlin, 2015. pp. 42

[51] S. Danjou. “Mehrzieloptimierung der Bauteilorientierung für Anwendungen der Rapid-Technologie “1st Edition, Cuvillier Verlag, 2010. pp. 121

[52] S. Danjou, and P. Köhler. "Determination of optimal build direction for different rapid prototyping applications." Proceedings of the 14th European forum on rapid prototyping. Ecole Centrale Paris, 2009. pp. 132.

[53] B. Vayre, F. Vignat, and F. Villeneuve. "Designing for additive manufacturing." Procedia CIRP vol. 3, pp. 632-637, 2012.

[54] L. E. Murr, et al. “Characterization of Ti6Al4V open cellular foams fabricated by additive manufacturing using electron beam melting,” Materials Science and Engineering: A, vol. 527 no. 7, pp. 1861- 1868, 2010.

[55] K. H. Shin, H. Natu, D. Dutta, J. Mazumder. “A method for the design and fabrication of heterogeneous objects”, Materials & Design, vol. 24, no. 5 pp. 339-353, 2003.

[56] C. Leyens, and M. Peters, eds. “Titanium and titanium alloys: fundamentals and applications.” John Wiley & Sons, pp.333-350, 2003.

[57] F. Memu, et al. "Effect of Surface Roughness on Tensile Properties of Electron Beam Melted Ti-6Al-4V Alloy." Euro PM 2019 Congress and Exhibition. European Powder Metallurgy Association (EPMA), October 13-16, 2019.

[58] B. Vayssette, N. Saintier, C. Brugger, M. Elmay, E. Pessard. “Surface roughness of Ti6Al-4V parts obtained by SLM and EBM: effect on the high cycle fatigue life”, Procedia Engineering, vol. 213, pp. 89-97, 2018.

[59] AP&C Ge Additive Company, “Ti-6Al-4V gr.5 Advanced Powders. “Advanced Powders, https://www.advancedpowders.com/powders/titanium/ti-6al-4v-5 (Accessed: July. 1, 2022)

[60] K. Mills, et al. "ASM handbook volume 9: metallography and microstructures." Metals Park, Ohio, USA: American Society for Metal, 1985. pp. 23-65

[61] R. Pederson. “Microstructure and phase transformation of Ti-6Al-4V.” Licentiate dissertation, Luleå tekniska universitet, 2002. pp. 10-29.

[62] M. Spiret, "The Definitive Guide to ASTM E8/E8M Tension Testing of Metals "Instron, https://www.instron.com/en/testing-solutions/astm-standards/the-definitive-guide-to-astm-e8-e8m (Accessed: July. 1, 2022)

[63] M. Guden. “Katmalı Malzemelerde Gerilme Dalgası Geçişinin Deneysel ne Nümerik Yöntemlerle Belirlenmesi: Hopkinson Basınç Bar Deneyleri.” İzmir Yüksek Teknoloji Enstitüsü, December, 2015. DOI:10.13140/RG.2.1.1926.5365.

[64] F. Yuan, V. Prakash, and T. Tullis. "Origin of pulverized rocks during earthquake fault rupture." Journal of Geophysical Research: Solid Earth vol. 116 no. 6, pp 1-18, 2011, DOI:10.1029/2010JB007721.

[65] A. M. Lennon, and K. T. Ramesh. "A technique for measuring the dynamic behavior of materials at high temperatures." International Journal of Plasticity vol. 14, no. 12, pp. 1279-1292, 1998.

[66] T. Bjerke, Z. Li, and J. Lambros. "Role of plasticity in heat generation during high-rate deformation and fracture of polycarbonate." International Journal of Plasticity vol. 18, no. 4, pp. 549-567, 2002.

[67] A. Kara, A. Tasdemirci, M. Guden. “Modeling quasi-static and high strain rate deformation and failure behavior of a (±45) symmetric E-glass/polyester composite under compressive loading.” Materials and Design, vol. 49, pp. 566-574, 2013.

[68] G. Ravichandran, G. Subhash. “Critical appraisal of limiting strain rates for compression testing of ceramics in a split Hopkinson pressure bar.” Journal of the American Ceramic Society, vol .77, pp. 263–267, 1994.

[69] T. Zhou, et al. "Dynamic shear characteristics of titanium alloy Ti-6Al-4V at large strain rates by the split Hopkinson pressure bar test." International Journal of Impact Engineering vol. 109, pp. 167-177, 2017.

[70] Q. S. Wu. “Effect of temperature and strain rate on mechanical behaviors of low alloy steel.” Journal of Materials Science-Materials in Electronics, vol. 3, no. 3, pp. 232-243, 2015.

[71] REL. “SHPB Compression System.” relinc, https://www.relinc.com/compression. (Accessed: July. 1, 2022)